Adolescent Alcohol Exposure Promotes Mechanical Allodynia and Alters Synaptic Function at Inputs from the Basolateral Amgydala to the Prelimbic Cortex

J. Daniel Obray[1], Erik T. Wilkes[1], Michael D. Scofield[1,2], and L. Judson Chandler[1]

[1]Department of Neuroscience, Medical University of South Carolina, Charleston, SC, 29425

[2]Department of Anesthesia and Perioperative Medicine, Medical University of South Carolina, Charleston, SC, 29425

Corresponding Author:
L. Judson Chandler, PhD
Department of Neuroscience
Medical University of South Carolina
30 Courtenay St
Charleston, SC 29425
Email: chandj@musc.edu

Abstract

Binge drinking is common among adolescents despite mounting evidence linking it to various adverse health outcomes that includes heightened pain perception. The prelimbic (PrL) cortex is vulnerable to insults from adolescent alcohol exposure and receives input from the basolateral amygdala (BLA) while sending projections to the ventrolateral periaqueductal gray (vlPAG) - two brain regions implicated in nociception. In this study, adolescent intermittent ethanol (AIE) exposure was carried out in male and female rats using a vapor inhalation procedure. Mechanical and thermal sensitivity, assessed throughout adolescence and into adulthood, revealed that AIE exposure induced protracted mechanical allodynia in both male and female rats. However, a carrageenan inflammatory paw pain challenge in adult rats revealed that AIE did not further augment carrageenan-induced hyperalgesia. To investigate synaptic function at BLA inputs onto defined populations of PrL neurons, retrobeads and viral labelling were combined with optogenetics and slice electrophysiology. Recordings from retrobead labelled cells in the PrL revealed AIE reduced BLA driven feedforward inhibition of neurons projecting from the PrL to the vlPAG (PrL^{PAG} neurons), resulting in augmented excitation/inhibition (E/I) balance and increased intrinsic excitability. Consistent with this finding, recordings from virally tagged PrL parvalbumin interneurons (PVINs) demonstrated that AIE exposure reduced both E/I balance at BLA inputs onto PVINs and PVIN intrinsic excitability when assessed in adulthood. These findings provide compelling evidence that AIE and acute pain alter synaptic function and intrinsic excitability within a prefrontal nociceptive circuit.

1. Introduction

Alcohol misuse and pain exhibit a bidirectional relationship. Due to its analgesic properties, alcohol is often used to self-medicate for pain relief[1,2]. However, the dose required for this effect results in blood alcohol levels akin to binge drinking[3,4], heightening the risk of alcohol related harm. While acute alcohol consumption can temporarily alleviate pain, chronic misuse promotes hyperalgesia[5-10]. Notably, frequent acute pain and pain interference are associated with an elevated risk of being diagnosed with an alcohol use disorder (AUD)[11-13]. This dynamic extends to adolescents where untreated pain correlates with earlier initiation of alcohol use[14], and alcohol consumption is associated with heightened ongoing and future pain[15-17]. Recent preclinical studies in rodents further indicate that adolescent intermittent ethanol (AIE) exposure induces persistent hyperalgesia spanning into adulthood[18-21]. Given the association between pain and AUD, understanding the impact of adolescent alcohol use on nociceptive circuits is crucial for improving AUD treatments.

Nociception involves multimodal processing across a distributed brain network. Within this network, the medial prefrontal cortex (mPFC) is a key node for evaluating and responding to pain[22-24]. The prelimbic (PrL) subregion of the mPFC receives inputs from the basolateral amygdala (BLA)[25-27] and sends projections to the ventrolateral periaqueductal gray (vlPAG)[28,29], both regions involved in nociception. Within this circuit, glutamatergic inputs from the BLA drive parvalbumin interneuron (PVIN) mediated feedforward inhibition of pyramidal neurons projecting from the PrL to the vlPAG (PrL^{PAG} neurons) to promote nociception[30-34]. Of note, activation of PrL PVINs has been shown to be pronociceptive[35,36], while activation of PrL^{PAG} neurons generally exhibits antinociceptive effects[32,36-38], although this finding has not been universally observed[39]. These findings highlight the involvement of a BLA-PrL-vlPAG circuit in modulating nociception.

Adolescence marks a critical period of continuing development for the mPFC. This period is characterized by heightened plasticity rendering this region particularly vulnerable to environmental insults, including those arising from binge alcohol consumption[40-42]. Notably, this developmental phase is accompanied by significant alterations in excitatory and inhibitory neurotransmission within the mPFC. Excitatory changes include pruning of both synapses and dendritic spines[43-47], maturation of AMPA and NMDA receptor trafficking[48-50], and increased innervation from the BLA[25,51]. Concurrently, there is a substantial increase in excitatory input onto PVINs[51,52], leading to a shift toward inhibition in the excitation/inhibition (E/I) balance at pyramidal neurons[53-55]. Preclinical rodent models have demonstrated that adolescent intermittent ethanol (AIE) exposure disrupts the normative developmental trajectory of the mPFC, inducing persistent alterations in intrinsic excitability and synaptic function. Specifically, AIE exposure leads to decreased intrinsic excitability of PVINs[56], reduced excitatory input onto PVINs[56], diminished inhibition at pyramidal neurons[57], and augmented intrinsic excitability of pyramidal neurons in the mPFC[58,59]. These findings underscore the sensitivity of mPFC circuitry to long-lasting AIE-induced changes. Building upon this understanding, the present study investigated how AIE exposure, in conjunction with a carrageen-induced inflammatory paw pain challenge, alters synaptic function at BLA inputs onto PVINs and Prl^{PAG} neurons.

2. Materials and Methods

2.1. Animals

Parvalbumin-Cre rats on a Long-Evans background were obtained from the Rat Resource and Research Center (line #00773) and bred to establish a colony at the Medical University of South Carolina. Rats were genotyped at postnatal day (PD) 14, with only hemizygote rats included in this study. On PD 21, rat pups were weaned, same sex group-housed (2-3 per cage) and assigned to one of four treatment groups: Air-saline (n = 30), Air-carrageenan (n = 30), AIE-saline (n = 30), or AIE-carrageenan (n = 29). Rats were housed in a temperature and humidity-controlled environment on a 12hr/12hr light/dark cycle, with lights off from 09:00-21:00 each day. Teklad 2918 (Envigo, Indianapolis, IN) chow and water were provided to the rats *ad libitum*. All procedures were carried out in accordance with the National Research Council's Guide for the Care and Use of Laboratory Animals (2011) and were approved by the Medical University of South Carolina Institutional Animal Care and Use Committee.

2.2. Adolescent Intermittent Ethanol Exposure

Adolescent intermittent ethanol exposure was carried out as previously described[60,61]. All rats underwent 8 cycles of intermittent ethanol vapor exposure beginning at PD 28 and continuing through PD 54. Each cycle consisted of two days of ethanol vapor exposure separated by two days of no ethanol exposure. The litter-matched Air rats received the same treatment except they were not exposed to ethanol vapor. On ethanol exposure days, rats were placed in the chambers at 18:00 and removed from the chambers at 08:00 on the following day. Upon removal from the chambers, the level of intoxication of each rat was rated on the following 5-point behavioral intoxication scale: 1 = no signs of intoxication; 2 = slightly intoxicated (slight motor impairment); 3 = moderately intoxicated (obvious motor impairment but able to walk); 4 = highly intoxicated (dragging abdomen, loss of righting reflex); 5 = extremely intoxicated (loss of righting reflex, and loss of eye blink reflex) [60,62,63]. On the last day of each cycle, blood was collected from the tail vein and analyzed for blood ethanol concentration (BEC) using an Analox alcohol analyzer (AM1, Analox Instruments, Stourbridge, GBR). Following the last exposure cycle, the rats remained group housed in the vivarium until undergoing surgery at ~ PD 80, after which they were single housed until being sacrificed to obtain slices for experimental use.

2.3. Stereotaxic Surgery

Rats undergoing stereotaxic surgery were induced and maintained under a surgical plane of anesthesia using isoflurane (2-3%). Intracranial injections were performed on a Kopf rat stereotaxic instrument (Kopf Instruments, Tujunga, CA, USA). A Micro4 (World Precision Instruments [WPI], Sarasota, FL, USA) controlled UMP3 microinjection pump (WPI) connected to a glass syringe (80100, Hamilton Company, Reno, NV) under stereotaxic control was used to inject 500 nl green retrobeads IX (Lumafluor Inc., Durham, NC) into the left vlPAG (from bregma: -8.4 mm AP, -0.7 mm ML, -6.3 mm DV), 500 nl of AAV5-hSyn-hChR2(H134R)-EYFP (26973-AAV5, Addgene, Watertown, MA) into the left BLA (from bregma: -2.7 mm AP, -5.1 mm ML, -8.8 mm DV), and 750 nl of AAV2-hSyn-DIO-mCherry (50459-AAV2, Addgene) into the left PrL cortex (from bregma: +2.8 mm AP, -0.6 mm ML, -3.8 mm DV). All injections occurred at 1 nl/s with the injector remaining in place for an additional 5 min following completion of the infusion. After surgery, a minimum of 4 weeks was given to allow the rats to recover and for retrograde transport and viral expression to occur.

2.4. Assessment of Mechanical and Thermal Sensitivity

Mechanical and thermal sensitivity were assessed using the electronic Von Frey and Hargreaves tests, respectively. Assessment began at PD 24 prior to initiation of ethanol vapor exposure on PD 28, and continued every 7 days until PD 80. Rats that subsequently underwent stereotaxic surgery followed by 4 wks of recovery, were reassessed for pain sensitivity. This was followed by injection with 100 µl of carrageenan (C2871, Tokyo Chemical Industry, Tokyo, JPN; 1% w/v in saline) or saline in the right hindpaw under brief isoflurane anesthesia. Subsequent pain sensitivity tests were conducted at 2 hr, 6 hr, and 24 hr post-injection, after which rats were sacrificed to obtain slices for experimental use.

Electronic Von Frey test for mechanical allodynia. On pain sensitivity test days, rats were placed in a 17" x 8.5" x 10" Plexiglas enclosure with a metal mesh floor. After a 5 min acclimation period, the mechanical sensitivity of the right hindpaw was assessed using an electronic Von Frey unit (38450, Ugo Basile, Gemonio, ITA). This consisted of placing the electronic Von Frey filament perpendicular to the plantar surface of the hindpaw and applying force until a sharp withdrawal response was elicited. Mechanical sensitivity was assessed three times per session for each rat and the average gram-force required to elicit a withdrawal response was recorded.

Hargreaves test for thermal hyperalgesia. Following assessment of allodynia, rats were placed in a 4" x 8" x 5.5" plexiglass enclosure with a glass floor. After a 15 min habituation period, the right hindpaw was stimulated using an infrared emitter from Ugo Basile (37570; 60% maximum intensity) and the latency to hindpaw withdrawal was measured. A 30 s cutoff was used to prevent tissue damage in rats that were unresponsive to the thermal stimulus. In each session the paw withdrawal latency was measured three times per rat and the average score was used to quantify the level of thermal sensitivity.

2.5. Electrophysiological Recordings

Acute slices were obtained from rats for electrophysiological recordings beginning at PD 110. Current clamp experiments were performed as previously described[56,64]. In brief, rats were anesthetized with isoflurane, and the brain was rapidly removed and placed into an ice-cold cutting solution containing (in mM): 93 NMDG, 2.5 KCl, 1.2 NaH_2PO_4, 30 $NaHCO_3$, 10 d-glucose, 20 HEPES, 2.5 $C_5H_9NO_3S$, 5 ascorbic acid, 15 sucrose, 10 $MgCl_2$, and 0.5 $CaCl_2$. Following sectioning using a Leica vibratome (VT 1200S, Wetzlar, DEU), 280 µM thick slices were incubated for at least 60 min at 34°C in artificial cerebrospinal fluid (aCSF) containing (in mM): 92 NaCl, 2.5 KCl, 1.2 NaH_2PO_4, 30 $NaHCO_3$, 10 d-glucose, 20 HEPES, 5 ascorbic acid, 10 $MgCl_2$, and 0.5 $CaCl_2$. After incubation, slices were transferred to a submerged recording chamber held at 34°C and constantly perfused with recording aCSF containing (in mM): 125 NaCl, 2.5 KCl, 25 $NaHCO_3$, 10 d-glucose, 0.4 ascorbic acid, 1.3 $MgCl_2$, and 2 $CaCl_2$. Each of these solutions was pH adjusted (pH 7.3-7.43), with an osmolarity of 300-310 mOsm, and was continuously aerated with 95% O_2/5% CO_2.

Recordings were performed using a Multiclamp 700B amplifier (Molecular Devices, San Jose, CA) connected to a Windows-PC running Axograph X software through an ITC-18 digital to analog converter (HEKA Instruments, Holliston, MA). A Sutter Instruments P-1000 micropipette puller (Novato, CA) was used to pull borosilicate glass electrodes. Tip resistances ranged from 4 to 8 MΩ. All recordings were obtained from visually identified green retrobead labelled PrL^{PAG} neurons or mCherry tagged PVINs in the left PrL. Cells were identified using a Zeiss Axio Examiner.A1 microscope (Oberkochen, DEU) equipped with a DIC filter and a filter for visualizing green retrobeads and mCherry. All internal solutions were adjusted to pH 7.4 and 285 mOsm. Series and membrane resistance were measured at the beginning and end of each recording, and if the series resistance exceeded 20 MΩ or changed by more than 10% then the cell was excluded from the analysis.

Current clamp recordings. Electrodes were filled with an internal solution containing (in mM): 125 potassium gluconate, 20 KCl, 10 HEPES, 1 EGTA, 2 $MgCl_2$, 2 Na_2-ATP, 0.3 Tris-GTP, and 10 phosphocreatine. To assess intrinsic excitability, picrotoxin (100 μM) and kynurenic acid (2 mM) were added to the perfused aCSF and 1 s current steps were applied in 20 pA increments ranging from -100 to +400 pA. Recordings were digitized at 10 kHz, filtered at 2 kHz, and analyzed for the number of action potentials elicited by each current step.

Voltage clamp recordings. Electrodes were filled with an internal solution containing (in mM): 125 cesium methanesulfonate, 10 CsCl, 4 NaCl, 10 HEPES, 1 EGTA, 2 $MgCl_2$, 2 Na_2-ATP, 0.5 Tris-GTP, 10 phosphocreatine, and 1 QX-314-Cl. All voltage clamp recordings were digitized at 10 kHz and filtered at 2 kHz. Postsynaptic events were evoked by optically stimulating channelrhodopsin expressing terminals from the BLA in the PrL cortex. This involved using Axograph to trigger a 5 ms pulse of light from an MDL-III-447 diode blue laser collimated to fit the microscope.

For experiments measuring the excitation/inhibition (E/I) balance of optically evoked postsynaptic currents onto PrL^{PAG} neurons and PrL PVINs, neurons were held at -70 mV for recordings of optically evoked excitatory postsynaptic currents (oEPSCs) and +10 mV for recordings of optically evoked inhibitory postsynaptic currents (oIPSCs). The peak amplitudes of the oEPSC and oIPSC events were analyzed, and their ratio (oEPSC/oIPSC) was computed.

For experiments measuring the AMPA/NMDA ratio at BLA inputs onto PrL^{PAG} and PrL PVINS, 1 μM tetrodotoxin (TTX) and 100 μM 4-aminopyridine (4-AP) were included in the aCSF to isolate monosynaptic transmission[65,66]. Neurons were held at +40 mV and optically evoked AMPA (oAMPA) and NMDA (oNMDA) currents were isolated using the following procedure: first, a combined oAMPA and oNMDA current was recorded in aCSF containing 100 μM picrotoxin. Subsequently, 50 μM dl-APV was added to the recording aCSF to isolate the oAMPA current. Finally, to isolate the oNMDA current, the oAMPA current was subtracted from the combined oAMPA and oNMDA current. The AMPA/NMDA ratio was then computed based on the amplitude of each current.

For experiments measuring optically evoked asynchronous EPSCs (aEPSCs), TTX (1 μM) and 4-AP (100 μM) were added to the recording aCSF and $SrCl_2$ (2 mM) was substituted for $CaCl_2$. The substitution of strontium for calcium induces asynchronous neurotransmitter release after the initial release event. The resulting interevent interval and amplitude of the asynchronous events are commonly used to quantify pre- and postsynaptic function within defined circuits[67-69]. Recordings of aEPSCs were collected from neurons voltage clamped at -70 mV and analyzed within a 400 ms window beginning 50 ms poststimulation.

2.6. Statistical Analyses

Statistical analyses were performed using Stata 15.1 (StataCorp LLC, College Station, TX). Data were assessed for normality using the Wilks-Shapiro test and checked for outliers using the IQR rule. The experimental unit for this study was the individual animal. As such, while electrophysiological measures (e.g. E/I balance, intrinsic excitability) were obtained from multiple neurons within each animal, the data were averaged within each animal prior to analysis and reporting. Unless otherwise indicated, all data were analyzed using analysis of variance (ANOVA) models including all relevant factors. Repeated measures analyses used the Greenhouse-Geisser correction for sphericity. Post-hoc tests were corrected for multiple comparisons using the Bonferroni method. All values reported are mean ± SEM. For purposes of statistical significance, $p < 0.05$ was considered significant.

3. Results

The procedure for adolescent alcohol exposure used in this study is a well characterized model designed to simulate the effects of repeated episodes of binge-like alcohol exposure. Rats were subjected to 8 intermittent cycles of ethanol vapor from PD 28-PD 54. Behavioral intoxication and BECs were assessed for each rat at the end of each cycle. The average behavioral intoxication score using the 5-point rating scale was 2.2 ± 0.1 for male rats in the AIE-saline treatment condition, 2.2 ± 0.1 for male rats in the AIE-carrageenan treatment condition, 2.2 ± 0.1 for female rats in the AIE-saline treatment condition, and 2.1 ± 0.1 for female rats in the AIE-carrageenan treatment condition, which represents a moderate level of intoxication. The corresponding BEC values were 196.4 ± 34.8 for male rats in the AIE-saline treatment condition, 240.0 ± 33.8 for male rats in the AIE-carrageenan treatment condition, 184.8 ± 38.8 for female rats in the AIE-saline treatment condition, and 177.7 ± 31.2 for female rats in the AIE-carrageenan treatment condition. Male rats had significantly higher intoxication scores than female rats (Wilcoxon rank-sum test: $z = 1.967$, $p = 0.0492$). There was no difference in average intoxication scores between rats assigned to the saline and carrageenan pain conditions (Wilcoxon rank-sum test: $z = 0.450$, $p = 0.6529$). There was no difference in BEC level between male and female rats (Wilcoxon rank-sum test: $z = 1.365$, $p = 0.1724$) or for rats assigned to the saline and carrageenan pain conditions (Wilcoxon rank-sum test: $z = -0.955$, $p = 0.3395$). Average intoxication scores and BEC levels were positively correlated ($r_s = 0.499$, $p = 0.001$).

3.1. Adolescent Intermittent Ethanol Exposure Augments Mechanical Sensitivity

The first set of studies evaluated the impact of AIE on mechanical and thermal sensitivity from adolescence to early adulthood. Weekly assessments were conducted using electronic Von Frey and Hargreaves apparatuses. The initial evaluation was performed at PD 24, prior to the first cycle of ethanol vapor exposure, while the final assessment took place at PD 80, approximately four weeks after the last cycle of exposure.

For mechanical sensitivity, analysis of data from the electronic Von Frey test revealed that AIE significantly reduced paw withdrawal threshold, indicating increased sensitivity to mechanical touch (main effect AIE: $F_{(1,115)} = 12.81$, $p = 0.0005$, partial $\eta^2 = 0.1002$ [0.0203, 0.2105]; **Fig. 1 A-B**). Additionally, female rats exhibited greater sensitivity to mechanical touch compared to male rats (main effect sex: $F_{(1,115)} = 5.98$, $p = 0.0160$, partial $\eta^2 = 0.0494$ [0.0014, 0.1434]). There was no significant interaction between AIE and sex (AIE x sex interaction: $F_{(1,115)} = 1.02$, $p = 0.3147$). Mechanical touch sensitivity decreased with age (main effect age: $F_{(8,920)} = 75.08$, $p = 0.0000$, partial $\eta^2 = 0.3950$, [0.3444, 0.4328]), with no significant interactions between age and AIE or sex (AIE x age interaction: $F_{(8,920)} = 0.70$, $p = 0.6327$; sex x age interaction: $F_{(8,920)} = 1.50$, $p = 0.1829$; AIE x sex x age interaction: $F_{(8,920)} = 1.10$, $p = 0.3602$). The data were also averaged for each rat starting after the first cycle of AIE (PD 31 – PD 80). Consistent with the full dataset analysis, the averaged data showed that AIE increased sensitivity to mechanical touch (main effect AIE: $F_{(1,115)} = 13.33$, $p = 0.0004$, partial $\eta^2 = 0.1039$ [0.0221, 0.2149]; **Fig. 1 C**) and female rats were more sensitive to mechanical touch than male rats (main effect sex: $F_{(1,115)} = 5.63$, $p = 0.0193$, partial $\eta^2 = 0.0467$ [0.0008, 0.1393]). There was no significant interaction between AIE and sex (AIE x sex interaction: $F_{(1,115)} = 1.28$, $p = 0.2608$).

For thermal sensitivity, analysis of data from the Hargreaves test indicated no significant effect of AIE on paw withdrawal latency (main effect AIE: $F_{(1,115)} = 1.21$, $p = 0.2738$; **Fig. 1 D-E**). Additionally, there were no significant sex differences or interactions with AIE (main effect sex: $F_{(1,115)} = 0.59$, $p = 0.4446$; AIE x sex interaction: $F_{(1,115)} = 1.85$, $p = 0.1767$). Thermal sensitivity was found to decrease with age (main effect age: $F_{(8,920)} = 11.45$, $p = 0.0000$, partial $\eta^2 = 0.0906$ [0.0520, 0.1197]). Furthermore, no significant interactions between age and AIE or sex were observed (AIE x age interaction: $F_{(8,920)} = 1.11$, $p = 0.3567$; sex x age interaction: $F_{(8,920)} = 2.02$, $p = 0.0546$; AIE x sex x age interaction: $F_{(8,920)} = 0.70$, p

= 0.6626). The data were also analyzed as the average paw withdrawal latency for each rat beginning after the first cycle of AIE (PD 31 – PD 80). Consistent with the results from the full dataset, analysis of the averaged data showed no significant effect of AIE, sex, or interaction between the two on thermal sensitivity (main effect AIE: $F_{(1,115)} = 1.09$, $p = 0.2977$; main effect sex: $F_{(1,115)} = 1.57$, $p = 0.2128$; AIE x sex interaction: $F_{(1,115)} = 2.20$, $p = 0.1408$; **Fig. 1 F**).

3.2. Carrageenan-Induced Inflammatory Paw Pain is Unaltered by Adolescent Intermittent Ethanol Exposure

As AIE was found to increase baseline mechanical sensitivity, the subsequent studies assessed its impact on carrageenan-induced hyperalgesia in adult rats. Carrageenan is a well-known proinflammatory agent that induces edema and transient hyperalgesia in the carrageenan-induced inflammatory paw pain model [70-74].

Prior to administering carrageenan or saline into the hindpaw, baseline mechanical and thermal sensitivity was assessed using the electronic Von Frey and Hargreaves tests, respectively. Analysis revealed that AIE driven reductions in paw withdrawal threshold persisted for more than eight weeks after discontinuing ethanol vapor exposure (main effect AIE: $F_{(1,109)} = 5.50$, $p = 0.0209$, partial $\eta^2 = 0.0480$ [0.0006, 0.1441]; **Fig. 2 A**). In addition, female rats continued to display greater mechanical sensitivity than males, with no significant interactions between AIE and sex (main effect sex: $F_{(1,109)} = 10.66$, $p = 0.0015$, partial $\eta^2 = 0.0891$ [0.0139, 0.1998]; AIE x sex interaction: $F_{(1,109)} = 0.93$, $p = 0.3367$). Baseline analysis of the thermal sensitivity data showed no significant effects of AIE, sex, or an interaction between AIE and sex on paw withdrawal latency (main effect AIE: $F_{(1,109)} = 1.69$, $p = 0.1968$; main effect sex: $F_{(1,109)} = 1.27$, $p = 0.2616$; AIE x sex interaction: $F_{(1,109)} = 0.38$, $p = 0.5384$; **Fig. 2 B**).

Following carrageenan or saline administration, mechanical and thermal sensitivity were evaluated, and data were averaged across assessments occurring at three timepoints – 2, 6, and 24 hr post-injection. The averaged data were expressed as a percentage of each rat's pre-injection baseline score. Examination of paw withdrawal threshold revealed a carrageenan-induced increase in mechanical sensitivity (main effect carrageenan: $F_{(1,105)} = 116.41$, $p = 0.0000$, partial $\eta^2 = 0.5258$ [0.3934, 0.6201]; **Fig. 2 C,E**). Analysis further indicated that female rats displayed a greater increase in sensitivity than males across both the saline and carrageenan treatments, with no significant effects of AIE, or interactions between AIE, sex, and carrageenan (main effect sex: $F_{(1,105)} = 6.22$, $p = 0.0142$, partial $\eta^2 = 0.0559$ [0.0020, 0.1578]; main effect AIE: $F_{(1,105)} = 0.93$, $p = 0.3366$; AIE x sex interaction: $F_{(1,105)} = 0.03$, $p = 0.8706$; AIE x carrageenan interaction: $F_{(1,105)} = 0.59$, $p = 0.4441$; sex x carrageenan interaction: $F_{(1,105)} = 1.72$, $p = 0.1925$; AIE x sex x carrageenan interaction: $F_{(1,105)} = 1.18$, $p = 0.2790$). Similarly, examination of paw withdrawal latency revealed a carrageenan-induced increase in thermal sensitivity (main effect carrageenan: $F_{(1,105)} = 132.70$, $p = 0.0000$, partial $\eta^2 = 0.5583$ [0.4308, 0.6470]; **Fig. 2 D,F**). No significant effects of AIE, sex, or interactions between AIE, sex, and carrageenan were observed (main effect AIE: $F_{(1,105)} = 0.00$, $p = 0.9625$; main effect sex: $F_{(1,105)} = 0.00$, $p = 0.9510$; AIE x sex interaction: $F_{(1,105)} = 0.23$, $p = 0.6307$; AIE x carrageenan interaction: $F_{(1,105)} = 0.01$, $p = 0.9352$; sex x carrageenan interaction: $F_{(1,105)} = 0.14$, $p = 0.7120$; AIE x sex x carrageenan interaction: $F_{(1,105)} = 3.85$, $p = 0.0524$).

3.3. Analysis of the Intrinsic Excitability of Prelimbic Neurons Projecting to the Ventrolateral Periaqueductal Gray

Subsequently, the impact of AIE exposure and carrageenan-induced hyperalgesia on PrL^{PAG} neuron intrinsic excitability was examined through current-clamp recordings of current evoked firing obtained from green retrobead labelled cells in the PrL cortex. Labelling with green retrobeads indicated that the neuron projected ipsilateral from the left hemisphere of the PrL cortex to the vlPAG

(**Fig. 3**). For each electrophysiological experiment, values are reported per animal and reflect the average value of 1-5 neurons recorded from each rat. **Table 1** contains a summary of the biophysical properties of the recorded PrL^{PAG} neurons. No significant differences between treatment conditions or sex were observed for these properties.

Analysis of the firing data indicated that both AIE and carrageenan enhanced intrinsic excitability (main effect AIE: $F_{(1,72)} = 7.26$, $p = 0.0088$, partial $\eta^2 = 0.0916$ [0.0060, 0.2295]; main effect carrageenan: $F_{(1,72)} = 4.07$, $p = 0.0475$, partial $\eta^2 = 0.0534$ [0.0000, 0.1775]; **Fig. 4 A-F**). Moreover, the effect of AIE on intrinsic excitability became more pronounced with increasing current step size (AIE x current step interaction: $F_{(20,1440)} = 3.83$, $p = 0.0115$, partial $\eta^2 = 0.0505$ [0.0195, 0.0606]). Although the number of action potentials fired increased alongside the amount of injected current (main effect of current step: $F_{(20,1440)} = 229.93$, $p = 0.0000$, partial $\eta^2 = 0.7615$ [0.7401, 0.7745]), no other significant effects of sex or interactions between AIE, carrageenan, sex, or current step were observed (main effect of sex: $F_{(1,72)} = 1.80$, $p = 0.1835$; AIE x carrageenan interaction: $F_{(1,72)} = 0.00$, $p = 0.9770$; AIE x sex interaction: $F_{(1,72)} = 0.16$, $p = 0.6864$; sex x carrageenan interaction: $F_{(1,72)} = 0.00$, $p = 0.9732$; AIE x sex x carrageenan interaction: $F_{(1,72)} = 0.45$, $p = 0.5027$; sex x current step interaction: $F_{(20,1440)} = 1.26$, $p = 0.2889$; carrageenan x current step interaction: $F_{(20,1440)} = 1.12$, $p = 0.3393$; AIE x sex x current step interaction: $F_{(20,1440)} = 0.65$, $p = 0.5801$; AIE x carrageenan x current step interaction: $F_{(20,1440)} = 2.44$, $p = 0.0681$; sex x carrageenan x current step interaction: $F_{(20,1440)} = 0.20$, $p = 0.8870$; AIE x sex x carrageenan x current step interaction: $F_{(20,1440)} = 1.11$, $p = 0.3460$).

3.4. Analysis of the Excitatory/Inhibitory Balance at Inputs from the Basolateral Amygdala onto Prelimbic Neurons Projecting to the Ventrolateral Periaqueductal Gray

The next set of studies assessed the impact of AIE and carrageenan on synaptic function at BLA inputs to PrL^{PAG} neurons. This involved recording from green retrobead labelled pyramidal neurons in the PrL cortex while optically stimulating terminals from the BLA.

To evaluate the E/I balance at BLA inputs to PrL^{PAG} neurons, voltage-clamp recordings of oEPSCs and oIPSCs were obtained from green retrobead labelled cells in the PrL. Analysis of oEPSC peak amplitudes indicated no significant effects of AIE, carrageenan, or sex (main effect AIE: $F_{(1,69)} = 2.36$, $p = 0.1294$; main effect of carrageenan: $F_{(1,69)} = 0.35$, $p = 0.5572$; main effect of sex: $F_{(1,69)} = 3.64$, $p = 0.0604$; AIE x carrageenan interaction: $F_{(1,69)} = 0.00$, $p = 0.9757$; AIE x sex interaction: $F_{(1,69)} = 1.45$, $p = 0.2334$; sex x carrageenan interaction: $F_{(1,69)} = 0.00$, $p = 0.9617$; AIE x sex x carrageenan interaction: $F_{(1,69)} = 0.76$, $p = 0.3851$; **Fig. 5 A,E**).

Conversely, oIPSC amplitude was significantly reduced in AIE exposed rats (main effect AIE: $F_{(1,69)} = 37.66$, $p = 0.0000$, partial $\eta^2 = 0.3531$ [0.1771, 0.4942]; **Fig. 5 B,F**). Additionally, carrageenan was found to enhance oIPSC amplitude (main effect carrageenan: $F_{(1,69)} = 4.17$, $p = 0.0449$, partial $\eta^2 = 0.0570$ [0.0000, 0.1858]); however, this increase was attenuated in AIE exposed rats (AIE x carrageenan interaction: $F_{(1,69)} = 5.16$, $p = 0.0262$, partial $\eta^2 = 0.0696$ [0.0000, 0.2036]). No significant effects of sex, or interactions between sex and AIE or carrageenan on oIPSC amplitude were found (main effect sex: $F_{(1,69)} = 0.83$, $p = 0.3644$; AIE x sex interaction: $F_{(1,69)} = 2.90$, $p = 0.0929$; sex x carrageenan interaction: $F_{(1,69)} = 0.97$, $p = 0.3287$; AIE x sex x carrageenan interaction: $F_{(1,69)} = 1.84$, $p = 0.1788$).

To quantify the resulting E/I balance at PrL^{PAG} neurons, the ratios of oEPSCs to oIPSCs were compared. This revealed that AIE enhanced the E/I balance (main effect AIE: $F_{(1,69)} = 52.48$, $p = 0.0000$, partial $\eta^2 = 0.4320$ [0.2545, 0.5611]; **Fig. 5 C,G**) and female rats exhibited larger E/I ratios than male rats (main effect sex: $F_{(1,69)} = 5.21$, $p = 0.0255$, partial $\eta^2 = 0.0703$ [0.0000, 0.2045]). No significant effects of carrageenan or interactions between AIE, sex, and carrageenan were found (main effect

carrageenan: $F_{(1,69)} = 0.96$, $p = 0.3307$; AIE x carrageenan interaction: $F_{(1,69)} = 0.01$, $p = 0.9158$; AIE x sex interaction: $F_{(1,69)} = 0.05$, $p = 0.8190$; sex x carrageenan interaction: $F_{(1,69)} = 1.72$, $p = 0.1935$; AIE x sex x carrageenan interaction: $F_{(1,69)} = 0.08$, $p = 0.7741$).

3.5. Analysis of AMPA and NMDA Currents at Direct Inputs from the Basolateral Amygdala onto Prelimbic Neurons Projecting to the Ventrolateral Periaqueductal Gray

To assess the AMPA/NMDA ratio at monosynaptic inputs from the BLA to PrL^{PAG} neurons, voltage-clamp recordings of oAMPA and oNMDA currents were obtained from green retrobead labelled cells in the PrL during application of TTX and 4-AP. Analysis of oAMPA current amplitude revealed no significant effects of AIE, carrageenan, or sex (main effect AIE: $F_{(1,72)} = 0.50$, $p = 0.4817$; main effect carrageenan: $F_{(1,72)} = 0.31$, $p = 0.5806$; main effect sex: $F_{(1,72)} = 3.19$, $p = 0.0784$; AIE x carrageenan interaction: $F_{(1,72)} = 0.03$, $p = 0.8652$; AIE x sex interaction: $F_{(1,72)} = 0.20$, $p = 0.6576$; sex x carrageenan interaction: $F_{(1,72)} = 0.29$, $p = 0.5889$; AIE x sex x carrageenan interaction: $F_{(1,72)} = 0.26$, $p = 0.6122$; **Fig. 6 A,E**). Likewise, evaluation of the amplitude of oNMDA currents revealed no effects of treatment condition or sex (main effect AIE: $F_{(1,72)} = 1.25$, $p = 0.2680$; main effect carrageenan: $F_{(1,72)} = 0.29$, $p = 0.5932$; main effect sex: $F_{(1,72)} = 2.86$, $p = 0.0952$; AIE x carrageenan interaction: $F_{(1,72)} = 0.34$, $p = 0.5635$; AIE x sex interaction: $F_{(1,72)} = 0.42$, $p = 0.5204$; sex x carrageenan interaction: $F_{(1,72)} = 1.55$, $p = 0.2176$; AIE x sex x carrageenan interaction: $F_{(1,72)} = 2.40$, $p = 0.1257$; **Fig. 6 B,F**). The resultant ratios of oAMPA to oNMDA currents were compared and also were found to be unaltered by AIE, carrageenan, or sex (main effect AIE: $F_{(1,72)} = 1.34$, $p = 0.2513$; main effect carrageenan: $F_{(1,72)} = 1.00$, $p = 0.3199$; main effect sex: $F_{(1,72)} = 2.81$, $p = 0.0982$; AIE x carrageenan interaction: $F_{(1,72)} = 0.25$, $p = 0.6173$; AIE x sex interaction: $F_{(1,72)} = 0.75$, $p = 0.3907$; sex x carrageenan interaction: $F_{(1,72)} = 0.01$, $p = 0.9328$; AIE x sex x carrageenan interaction: $F_{(1,72)} = 1.30$, $p = 0.2582$; **Fig. 6 C,G**).

3.6. Analysis of Asynchronous Excitatory Postsynaptic Currents at Direct Inputs from the Basolateral Amygdala onto Prelimbic Neurons Projecting to the Ventrolateral Periaqueductal Gray

To examine pre- and postsynaptic alterations in glutamatergic neurotransmission at BLA inputs onto PrL^{PAG} neurons, voltage-clamp recordings of aEPSCs were obtained from green retrobead labelled cells while bath applying TTX and 4-AP. Analysis showed that female rats exhibited larger aEPSCs than male rats (main effect sex: $F_{(1,70)} = 11.75$, $p = 0.0010$, partial $\eta^2 = 0.1437$ [0.0256, 0.2925]). No other significant effects of AIE, carrageenan, or any interactions on aEPSC amplitude were observed (main effect AIE: $F_{(1,70)} = 0.25$, $p = 0.6200$; main effect carrageenan: $F_{(1,70)} = 0.08$, $p = 0.7733$; AIE x carrageenan interaction: $F_{(1,70)} = 0.24$, $p = 0.6239$; AIE x sex interaction: $F_{(1,70)} = 0.09$, $p = 0.7713$; sex x carrageenan interaction: $F_{(1,70)} = 3.62$, $p = 0.0613$; AIE x sex x carrageenan interaction: $F_{(1,70)} = 0.47$, $p = 0.4974$; **Fig. 7 A,D**). Likewise, assessment of the aEPSC interevent interval revealed no significant effects of AIE, carrageenan, or sex (main effect AIE: $F_{(1,70)} = 0.52$, $p = 0.4731$; main effect of carrageenan: $F_{(1,70)} = 0.01$, $p = 0.9106$; main effect of sex: $F_{(1,70)} = 0.03$, $p = 0.8678$; AIE x carrageenan interaction: $F_{(1,70)} = 0.15$, $p = 0.7021$; AIE x sex interaction: $F_{(1,70)} = 0.65$, $p = 0.4224$; sex x carrageenan interaction: $F_{(1,70)} = 2.39$, $p = 0.1265$; AIE x sex x carrageenan interaction: $F_{(1,70)} = 0.02$, $p = 0.8815$; **Fig. 7 B,E**).

3.7. Analysis of the Intrinsic Excitability of Prelimbic Parvalbumin Positive Interneurons

After observing altered inhibition of PrL^{PAG} neurons, the impact of AIE exposure and carrageenan-induced hyperalgesia on PrL PVIN intrinsic excitability was evaluated through current-clamp recordings of current evoked firing obtained from mCherry tagged cells in the PrL cortex. As expected, mCherry tagged neurons were distributed throughout layers II/III and V/VI in the PrL, with the highest concentration observed in layer V. **Table 2** contains a summary of the biophysical properties of the

recorded PVINs. No significant differences between treatment conditions or sex were observed for these properties.

Analysis of the firing of PrL PVINs revealed AIE reduced intrinsic excitability, with the magnitude of this reduction increasing with the amount of current injected (main effect AIE: $F_{(1,72)}$ = 5.46, p = 0.0222, partial η^2 = 0.0705 [0.0006, 0.2019]; AIE x current step interaction: $F_{(20,1440)}$ = 4.77, p = 0.0098, partial η^2 = 0.0621 [0.0289, 0.0744]; **Fig. 8 A-F**). Additionally, carrageenan enhanced the number of evoked action potentials at large but not small current steps, although the main effect was not significant (main effect carrageenan: $F_{(1,72)}$ = 2.27, p = 0.1360; carrageenan x current step interaction: $F_{(20,1440)}$ = 3.58, p = 0.0304, partial η^2 = 0.0473 [0.0170, 0.0567]). There were no significant effects of sex, or interactions between treatment conditions, sex, and current step (main effect sex: $F_{(1,72)}$ = 0.00, p = 0.9832; AIE x carrageenan interaction: $F_{(1,72)}$ = 0.09, p = 0.7628; AIE x sex interaction: $F_{(1,72)}$ = 0.17, p = 0.6823; sex x carrageenan interaction: $F_{(1,72)}$ = 0.01, p = 0.9147; AIE x sex x carrageenan interaction: $F_{(1,72)}$ = 0.00, p = 0.9919; sex x current step interaction: $F_{(20,1440)}$ = 0.44, p = 0.6444; AIE x sex x current step interaction: $F_{(20,1440)}$ = 0.81, p = 0.4464; AIE x carrageenan x current step interaction: $F_{(20,1440)}$ = 0.65, p = 0.5222; sex x carrageenan x current step interaction: $F_{(20,1440)}$ = 0.25, p = 0.7765; AIE x sex x carrageenan x current step interaction: $F_{(20,1440)}$ = 0.43, p = 0.6510). However, the number of current evoked action potentials increased with the amount of current injected (main effect current step: $F_{(20,1440)}$ = 181.42, p = 0.000, partial η^2 = 0.7159 [0.6907, 0.7311]).

3.8. Analysis of the Excitation/Inhibition Balance at Inputs from the Basolateral Amygdala onto Prelimbic Parvalbumin Positive Interneurons

After assessing the intrinsic excitability of PVINs, the next set of experiments characterized the impact of AIE exposure and carrageenan-induced hyperalgesia on synaptic function at BLA inputs to PrL PVINs. This involved recording from mCherry tagged PVINs in the PrL cortex while optically stimulating terminals from the BLA.

To evaluate the E/I balance at BLA inputs to PVINs, voltage-clamp recordings of oEPSCs and oIPSCs were obtained from mCherry tagged neurons in the PrL. Analysis revealed that AIE significantly reduced oEPSC amplitude (main effect AIE: $F_{(1,72)}$ = 14.80, p = 0.0003, partial η^2 = 0.1705 [0.0409, 0.3194]; **Fig. 9 A,E**), with larger oEPSCs in females than males (main effect sex: $F_{(1,72)}$ = 8.22, p = 0.0054, partial η^2 = 0.1025 [0.0094, 0.2429]). No significant effects of carrageenan, or interactions between AIE, carrageenan, or sex were observed (main effect of carrageenan: $F_{(1,72)}$ = 1.33, p = 0.2520; AIE x carrageenan interaction: $F_{(1,72)}$ = 0.08, p = 0.7839; AIE x sex interaction: $F_{(1,72)}$ = 0.26, p = 0.6126; sex x carrageenan interaction: $F_{(1,72)}$ = 0.41, p = 0.5254; AIE x sex x carrageenan interaction: $F_{(1,72)}$ = 0.26, p = 0.6110).

Examination of oIPSC amplitudes uncovered a significant AIE x sex interaction (AIE x sex interaction: $F_{(1,72)}$ = 4.48, p = 0.0377, partial η^2 = 0.0586 [0.0000, 0.1851]; **Fig. 9 B,F**), but no further significant effects of AIE, carrageenan, or sex (main effect AIE: $F_{(1,72)}$ = 0.00, p = 0.9927; main effect carrageenan: $F_{(1,72)}$ = 0.16, p = 0.6871; main effect sex: $F_{(1,72)}$ = 0.14, p = 0.7094; AIE x carrageenan interaction: $F_{(1,72)}$ = 1.15, p = 0.2867; sex x carrageenan interaction: $F_{(1,72)}$ = 0.19, p = 0.6673; AIE x sex x carrageenan interaction: $F_{(1,72)}$ = 0.07, p = 0.7895). Subsequent post hoc analysis did not find significant effects of AIE in male (t = 1.49, p = 0.281) or female (t = -1.50, p = 0.274) rats nor did it find significant sex differences in Air (t = 1.23, p = 0.443) or AIE exposed (t = -1.76, p = 0.165) rats.

Comparisons of oEPSCs to oIPSCs ratios to evaluate the E/I balance indicated larger ratios in females compared to males (main effects sex: $F_{(1,72)}$ = 12.12, p = 0.0009, partial η^2 = 0.1440 [0.0269, 0.2909]; **Fig. 9 C,G**). Additionally, AIE reduced the E/I ratio, with a more pronounced reduction

observed in males than in females (main effect AIE: $F_{(1,72)}$ = 15.60, p = 0.0002, partial η^2 = 0.1781 [0.0453, 0.3273]; AIE x sex interaction: $F_{(1,72)}$ = 4.64, p = 0.0345, partial η^2 = 0.0606 [0.0000, 0.1880]). In contrast, carrageenan augmented the E/I balance (main effect carrageenan: $F_{(1,72)}$ = 7.48, p = 0.0079, partial η^2 = 0.0941 [0.0067, 0.2326]). No further significant interactions between AIE, carrageenan, and sex were observed (AIE x carrageenan interaction: $F_{(1,72)}$ = 1.48, p = 0.2278; sex x carrageenan interaction: $F_{(1,72)}$ = 0.57, p = 0.4523; AIE x sex x carrageenan interaction: $F_{(1,72)}$ = 0.12, p = 0.7347).

3.9. Analysis of AMPA and NMDA Currents at Direct Inputs from the Basolateral Amygdala onto Prelimbic Parvalbumin Positive Interneurons

To assess the AMPA/NMDA ratio at monosynaptic BLA inputs onto PrL PVINs, voltage-clamp recordings of oAMPA and oNMDA currents were obtained from mCherry tagged neurons in the PrL cortex during bath application of TTX and 4-AP. Analysis revealed that AIE exposure attenuated oAMPA current amplitude, whereas carrageenan enhanced it (main effect AIE: $F_{(1,72)}$ = 8.67, p = 0.0043, partial η^2 = 0.1075 [0.0112, 0.2490]; main effect carrageenan: $F_{(1,72)}$ = 8.55, p = 0.0046, partial η^2 = 0.1062 [0.0107, 0.2474]; **Fig. 10 A,E**). No significant effects of sex or any interactions were observed (main effect sex: $F_{(1,72)}$ = 0.13, p = 0.7202; AIE x carrageenan interaction: $F_{(1,72)}$ = 1.33, p = 0.2533; AIE x sex interaction: $F_{(1,72)}$ = 0.56, p = 0.4549; sex x carrageenan interaction: $F_{(1,72)}$ = 0.31, p = 0.5783; AIE x sex x carrageenan interaction: $F_{(1,72)}$ = 0.09, p = 0.7650).

Similarly, the amplitude of oNMDA currents was reduced by AIE (main effect AIE: $F_{(1,72)}$ = 7.32, p = 0.0085, partial η^2 = 0.0923 [0.0062, 0.2303]; **Fig. 10 B,F**). However, neither carrageenan nor sex, nor any interaction between AIE, carrageenan, or sex was observed to impact oNMDA currents (main effect carrageenan: $F_{(1,72)}$ = 0.08, p = 0.7814; main effect sex: $F_{(1,72)}$ = 1.69, p = 0.1971; interaction AIE x carrageenan: $F_{(1,72)}$ = 2.37, p = 0.1279; interaction AIE x sex: $F_{(1,72)}$ = 0.04, p = 0.8458; interaction sex x carrageenan: $F_{(1,72)}$ = 1.80, p = 0.1836; interaction AIE x sex x carrageenan: $F_{(1,72)}$ = 0.10, p = 0.7493).

After analyzing the oAMPA and oNMDA currents individually, ratios of oAMPA to oNMDA currents were compared. This revealed that carrageenan significantly enhanced the AMPA/NMDA ratio (main effect carrageenan: $F_{(1,72)}$ = 6.70, p = 0.0116, partial η^2 = 0.0852 [0.0042, 0.2213]; **Fig. 10 C,G**). The analysis also uncovered a trend toward a significant interaction between AIE and carrageenan, reflecting a nearly significant reduction of the effect of carrageenan in AIE exposed rats (AIE x carrageenan interaction: $F_{(1,72)}$ = 3.97, p = 0.0501). No additional significant effects were detected (main effect AIE: $F_{(1,72)}$ = 0.39, p = 0.5330; main effect sex: $F_{(1,72)}$ = 0.19, p = 0.6635; AIE x sex interaction: $F_{(1,72)}$ = 0.50, p = 0.4814; sex x carrageenan interaction: $F_{(1,72)}$ = 2.49, p = 0.1191; AIE x sex x carrageenan interaction: $F_{(1,72)}$ = 0.00, p = 0.9547).

3.10. Analysis of Asynchronous Excitatory Postsynaptic Currents at Direct Inputs from the Basolateral Amygdala onto Prelimbic Parvalbumin Positive Interneurons

To assess pre- and postsynaptic changes in glutamatergic neurotransmission at direct inputs from the BLA onto PVINs in the PrL cortex, voltage-clamp recordings were acquired from mCherry tagged neurons during bath application of TTX and 4-AP. Analysis revealed an AIE-induced reduction in amplitude (main effect AIE: $F_{(1,71)}$ = 17.60, p = 0.0001, partial η^2 = 0.1986 [0.0572, 0.3493]; **Fig. 11 A,D**). No additional effects of carrageenan, sex, or interactions between treatment condition and sex were detected (main effect carrageenan: $F_{(1,71)}$ = 0.15, p = 0.6961; main effect sex: $F_{(1,71)}$ = 1.38, p = 0.2441; AIE x carrageenan interaction: $F_{(1,71)}$ = 0.10, p = 0.7556; AIE x sex interaction: $F_{(1,71)}$ = 0.44, p = 0.5115; sex x carrageenan interaction: $F_{(1,71)}$ = 1.89, p = 0.1733; AIE x sex x carrageenan interaction: $F_{(1,71)}$ = 0.00, p = 0.9505). In contrast, evaluation of the interevent interval revealed female rats had smaller interevent intervals than male rats (main effect sex: $F_{(1,71)}$ = 8.44, p = 0.0049, partial η^2 =

0.1062 [0.0104, 0.2484]; **Fig. 11 B,E**), while finding no additional significant effects of AIE, carrageenan, or interactions between treatment conditions and sex (main effect AIE: $F_{(1,71)} = 0.51$, $p = 0.4795$; main effect carrageenan: $F_{(1,71)} = 1.05$, $p = 0.3079$; AIE x carrageenan interaction: $F_{(1,71)} = 1.00$, $p = 0.3196$; AIE x sex interaction: $F_{(1,71)} = 0.46$, $p = 0.5009$; sex x carrageenan interaction: $F_{(1,71)} = 0.00$, $p = 0.9530$; AIE x sex x carrageenan interaction: $F_{(1,71)} = 0.29$, $p = 0.5943$).

4. Discussion

Emerging evidence from preclinical rodent models indicates that AIE exposure induces long-lasting hyperalgesia[18-21]. While changes within extended amygdala circuitry contribute to altered nociception in AIE exposed animals[19-21], the impact on prefrontal nociceptive circuits remains unexplored. This study investigated the effects of AIE exposure and carrageenan-induced inflammatory paw pain on synaptic function and intrinsic excitability within a BLA-PrL-vlPAG circuit involved in modulating the descending pain pathway. The central finding was that AIE enhanced mechanical allodynia, and that this enhancement was accompanied by altered E/I balance and intrinsic excitability at PrL^{PAG} neurons and PVINs. Carrageenan-induced hyperalgesia was unaltered by AIE exposure while pain-induced plasticity at BLA inputs to PrL PVINs was reduced.

In this study, mechanical and thermal sensitivity were assessed from adolescence to early adulthood using the electronic Von Frey and Hargreaves tests. Mechanical sensitivity was heightened in both male and female rats exposed to AIE, consistent with previous findings in rodents[18-21]. While AIE induced significant mechanical hypersensitivity, thermal sensitivity remained unchanged. Although this contrasts with previous research[18,20], for female rats this difference may be due, at least in part, to different statistical approaches for analysis of the data. In the present study, sex was included as a between-subjects factor in the ANOVA whereas in the prior study data were analyzed separately for male and female rats. Consistent with this, when we analyzed our male and female data separately, we did observe a transient increase in thermal sensitivity in female rats as was reported previously[20]. Discrepancies regarding the impact of AIE on thermal sensitivity in males may stem from methodological differences such as the use of different strains of rats and differences in the ethanol exposure paradigms.

We next examined whether AIE exposure would amplify carrageenan-induced hyperalgesia in adult rats. Following an injection with carrageenan, both mechanical and thermal paw withdrawal thresholds decreased significantly. Adolescent intermittent ethanol exposure did not materially alter carrageenan-induced hyperalgesia, contrary to a previous observations with formalin[20] and sickness syndrome induced hyperalgesia[75]. Methodological differences in the choice of hyperalgesia inducing compounds, pain assays, and the duration of time between AIE exposure and the pain challenge may explain this discrepancy.

After assessing the effects of AIE exposure on carrageenan-induced pain, patch-clamp slice electrophysiology was performed to assess intrinsic excitability and synaptic function within the BLA-PrL-vlPAG circuit. For PrL^{PAG} neurons, these experiments revealed that AIE increased intrinsic excitability. Previous research has shown either unchanged[56,59,76] or increased intrinsic excitability of PrL pyramidal neurons following AIE[58,59]. Notably, the maximum current injected in the present study was larger than that used in studies which detected no effect of AIE on intrinsic excitability and closely matched that of studies which had reported increased intrinsic excitability. Thus, it is possible that the size of the largest current steps is a key determinant as to whether changes in intrinsic excitability are detected. Alternatively, AIE may produce projection specific changes in intrinsic excitability.

Increased intrinsic excitability of PrL^{PAG} neurons was accompanied by augmented E/I balance in AIE exposed rats. The increased E/I balance resulted from reduced oIPSC amplitude. This indicated that AIE exposure reduced PVIN mediated feedforward inhibition of PrL^{PAG} neurons by inputs from the BLA. This is an interesting observation as it suggests that AIE prevents the normal developmental shift toward greater inhibition at PrL pyramidal neurons that occurs as PVINs mature during adolescence[52-54,77].

To investigate the change in feedforward inhibition, we conducted electrophysiological recordings from PrL PVINs. These recordings revealed significantly reduced intrinsic excitability in AIE exposed animals, consistent with previous reports[56]. Notably, PVIN intrinsic excitability is developmentally regulated and increases during adolescence[78]. Decreased intrinsic excitability coincided with reduced BLA driven E/I balance at PrL PVINs in male AIE exposed rats, with an attenuated effect in females. The reduced E/I balance primarily stemmed from a decrease in oEPSC amplitude, although AIE did alter oIPSC amplitude in a sex-dependent manner. The sex-dependent effect of AIE on oIPSCs is difficult to interpret, as post-hoc tests did not reveal any significant effects. However, visual inspection of the data suggests a potential trend toward increased oIPSC amplitude in male AIE exposed rats and reduced amplitude in females. Intriguingly, AIE exposure elicits sex-dependent effects on PrL somatostatin interneuron intrinsic excitability[79]. As these neurons receive inputs from the BLA[30,80] and project to PrL PVINs[80], it is possible that somatostatin neurons are responsible for the sex-dependent effects of AIE on E/I balance and oIPSCs at PVINs.

To better characterize the reduction in glutamate signaling, we next measured monosynaptic oAMPA and oNMDA currents at BLA inputs onto PVINs. This revealed that AIE significantly decreased oAMPA and oNMDA currents without altering the overall AMPA/NMDA ratio. This agreed with prior research from our lab which found AIE reduced electrically evoked AMPA and NMDA currents onto PVINs[56]. To determine whether this reduction resulted from pre- or postsynaptic changes, aEPSCs were recorded from PVINs in the PrL cortex. The amplitude but not the interevent interval of the aEPSCs was reduced in AIE exposed animals, indicating a reduction in postsynaptic receptor function. These findings provide strong evidence for reduced glutamate signaling efficacy at BLA inputs onto PVINs following AIE exposure.

These findings indicate that following AIE BLA dependent feedforward inhibition of PrL^{PAG} neurons is decreased. This results from decreased PrL PVIN intrinsic excitability and reduced postsynaptic glutamate receptor function at BLA inputs to PrL PVINs. Within the BLA-PrL-vlPAG circuit, PrL^{PAG} neuron activation is generally associated with antinociceptive effects[32,33,36-38], while PrL PVIN activation is associated with pronociceptive effects[35]. However, PrL^{PAG} neuron activation can be pronociceptive[39]. Notably, chronic activation of a PrL nociceptive ensemble including PrL^{PAG} neurons has been shown to induce a chronic pain-like behaviors[81]. As PrL^{PAG} neurons project to both GABA and glutamate neurons in the vlPAG[32,82], and these populations have been shown to be pro- and antinociceptive, respectively[83], the balance of PrL^{PAG} input onto these populations may determine the effect of PrL^{PAG} activation on nociception. While speculative, we hypothesize that AIE selectively strengthens the input from PrL^{PAG} neurons onto vlPAG GABA neurons, resulting in mechanical allodynia that could be alleviated by inhibiting PrL^{PAG} neurons or activating PrL PVINs. Alternatively, these changes could represent an antinociceptive compensatory response for pronociceptive changes in other nociceptive circuits. Future experiments could test these hypotheses.

The intrinsic excitability of PrL^{PAG} neurons was increased following a carrageenan-induced pain challenge, akin to the heightened excitability observed in AIE exposed rats. Intrinsic excitability is also enhanced in PrL pyramidal neurons 3-5 days after intraplantar injection with complete Freund's adjuvant[84]. Interestingly, in a chronic neuropathic pain model, the intrinsic excitability of PrL^{PAG} neurons decreases 7 days after a chronic constriction injury[85], suggesting a shift from increased to decreased excitability in the transition from acute to chronic pain states. In addition to enhancing the excitability of PrL^{PAG} neurons, we observed that carrageenan also increased the amplitude of oIPSCs in Air control rats, with a blunted effect in AIE exposed rats. Despite no change in glutamate transmission at BLA inputs onto PrL^{PAG} neurons, the E/I balance remained unaltered. These findings are similar to those seen in a kaolin-carrageenan arthritis model, where the amplitude of BLA driven

electrically evoked IPSCs (eIPSCs) onto PrL pyramidal neurons is significantly increased without a corresponding change in glutamate transmission[86]. These findings indicate that enhanced inhibitory transmission at PrL pyramidal neurons is a hallmark of carrageenan-induced inflammatory pain.

As in PrL^{PAG} neurons, carrageenan elevated the intrinsic excitability of PVINs, albeit only at large current steps. Accompanying this elevation was enhanced E/I balance at PVINs. There was not a significant change in either oEPSC or oIPSC amplitude, suggesting subtle alterations in both excitatory and inhibitory neurotransmission. The monosynaptic oAMPA current was enhanced at PrL PVINs, leading to an increase in the AMPA/NMDA ratio of Air control rats, with a weakened effect observed in AIE exposed rats. Surprisingly, the increased oAMPA currents at PVINs did not correspond to changes in either aEPSC amplitude or interevent interval. This leaves it unclear whether the observed change in synaptic strength resulted from a modification in presynaptic release probability or postsynaptic receptor function.

The present study demonstrates that in carrageenan-induced inflammatory pain, BLA inputs onto PVINs are strengthened. This strengthening, alongside increased PVIN excitability, enhances inhibition of PrL^{PAG} neurons. Notably, PrL^{PAG} neuron intrinsic excitability is increased, possibly to compensate for increased inhibitory input. Remarkably, the effects of carrageenan on synaptic function were blunted in AIE exposed rats, suggesting that AIE not only induces PVIN hypofunction, but also restricts pain-induced plasticity at PVINs. Intriguingly, AIE augments the number of PNN enwrapped PVINs in the PrL cortex[87]. As PNNs play a role in stabilizing synapses and restricting plasticity[88-90], this may reduce synaptic plasticity at PrL PVINs. Surprisingly, despite restricted plasticity at BLA inputs to PVINs, there were no AIE dependent changes in carrageenan-induced hyperalgesia.

5. Conclusion

In conclusion, the present study examined the effects of AIE exposure and a carrageenan pain challenge on a BLA-PrL-vlPAG circuit involved in modulating the descending pain pathway. Following AIE exposure, while rats displayed enhanced mechanical sensitivity, carrageenan-induced hyperalgesia was not altered by a history of AIE exposure. In AIE exposed rats, BLA inputs to the PrL were biased toward decreased PVIN mediated feedforward inhibition of PrL^{PAG} neurons. A carrageenan pain challenge increased BLA mediated inhibitory drive onto these neurons in Air control but not AIE exposed animals. These changes suggest that AIE induces long-lasting reductions in PVIN mediated feedforward inhibition of PrL^{PAG} neurons which accompany increased mechanical sensitivity. In addition to reduced feedforward inhibition, AIE may also diminish plasticity at PrL PVINs. Beyond the implications for nociception, these AIE-induced alterations in BLA-PrL-vlPAG function may impact other PrL^{PAG} neuron mediated behaviors such as context fear discrimination[91], passive avoidance[92], and arousal[82].

Acknowledgements

The authors would like to thank members of the Chandler Lab for their help carrying out the ethanol vapor exposure. This work was supported by NIH grants AA019967 (LJC), T32 AA007474 (JDO), and F32 AA030193 (JDO). The authors declare that the research was carried out in the absence of any commercial or financial relationships that could be construed as a conflict of interest. The artwork depicting electrophysiological recordings from PrL^{PAG} neurons and PVINs in figures 4-11 was drawn in part using images from Servier Medical Art. Servier Medical Art is licensed under a Creative Commons Attribution 4.0 Unported License (https://creativecommons.org/licenses/by/4.0/).

Table 1. Biophysical properties of PrL^{PAG} neurons across treatment condition and sex.

Condition	Sex	V_{rest} (mV)	R_{input} (MΩ)
AIR: Saline	Male	-66.6 ± 0.9	75.3 ± 3.5
	Female	-65.0 ± 1.7	76.3 ± 2.4
AIR: Carrageenan	Male	-66.2 ± 1.4	83.2 ± 5.4
	Female	-65.2 ± 1.5	83.9 ± 4.1
AIE: Saline	Male	-65.0 ± 1.4	86.9 ± 7.8
	Female	-65.6 ± 1.5	76.6 ± 2.9
AIE: Carrageenan	Male	-65.6 ± 1.0	88.6 ± 4.3
	Female	-66.5 ± 1.2	83.4 ± 6.0

Table 2. Biophysical properties of PVINs across treatment condition and sex.

Condition	Sex	V_{rest} (mV)	R_{input} (MΩ)
AIR: Saline	Male	-74.3 ± 1.9	145.1 ± 5.1
	Female	-72.6 ± 1.6	155.4 ± 8.8
AIR: Carrageenan	Male	-72.5 ± 1.9	138.1 ± 7.4
	Female	-73.7 ± 1.6	135.4 ± 8.9
AIE: Saline	Male	-73.6 ± 1.3	155.7 ± 4.9
	Female	-74.6 ± 1.8	147.0 ± 5.2
AIE: Carrageenan	Male	-71.6 ± 2.1	153.2 ± 8.3
	Female	-74.0 ± 1.6	141.3 ± 5.9

Figure Legends

Figure 1. Mechanical and thermal sensitivity of rats during adolescence and early adulthood. (**A,B**) Depiction of the effect of adolescent intermittent ethanol (AIE) exposure on mechanical sensitivity across adolescence and into early adulthood in male (**A**) and female (**B**) rats. (**C**) Adolescent intermittent ethanol exposure significantly reduced the average (PD 31-PD 80) electronic Von Frey (eVF) withdrawal threshold, indicating increased mechanical touch sensitivity. (**D,E**) Depiction of the effect of AIE exposure on thermal sensitivity from adolescence to early adulthood in male (**D**) and female (**E**) rats. (**F**) Adolescent intermittent ethanol exposure did not significantly alter the average (PD 31-PD 80) Hargreaves test withdrawal latency, indicating no change in thermal sensitivity. Data represent the mean ± SEM. *, indicates a significant difference between the related conditions; $p < 0.05$; n = 29-30 rats/group.

Figure 2. Mechanical and thermal sensitivity of rats in response to a carrageenan paw pain challenge. (**A**) Baseline mechanical touch sensitivity was greater in adolescent intermittent ethanol (AIE) exposed rats than in Air control rats. (**B**) There was no difference in baseline thermal sensitivity between AIE exposed and Air control rats. (**C,D**) Male rats injected with carrageenan (CAR) into the right hindpaw displayed hypersensitivity to both mechanical (**C**) and thermal (**D**) stimuli following the injection. This hypersensitivity was not significantly altered by AIE exposure. (**E,F**) Similarly, female rats injected with CAR into the right hindpaw displayed hypersensitivity to both mechanical (**E**) and thermal (**F**) stimuli, with no effect of AIE exposure on this hypersensitivity. Data represent the mean ± SEM. *, indicates a significant difference between the related conditions; $p < 0.05$; n = 13-15 rats/group.

Figure 3. Experimental approach. (**A**) Experimental timeline displaying the age of animals at each phase in the study. (**B**) Diagram showing the viral and retrobead labelling approach used to identify and manipulate specific neuronal populations in the prelimbic (PrL) cortex. (**C**) Representative images showing injection sites in the PrL (left panel, AAV2-hSyn-DIO-mCherry), basolateral amygdala (BLA, center panel, AAV5-hSyn-hChR2(H134R)-EYFP), and ventrolateral periaqueductal gray (vlPAG, right panel, green retrobeads). (**D**) Representative images from the PrL cortex (from left to right) of BLA terminals, mCherry tagged PVINs, and green retrobead labelled PrL^{PAG} neurons.

Figure 4. Intrinsic excitability of pyramidal neurons projecting from the prelimbic cortex to the ventrolateral periaqueductal gray (PrL^{PAG}). (**A**) Electrophysiological recordings were obtained from PrL^{PAG} neurons in the PrL cortex. (**B**) Depiction of the relationship between injected current and action potential firing in male rats across treatment conditions. (**C**) The cumulative number of action potentials fired across all current steps was increased by both adolescent intermittent ethanol (AIE) exposure and a carrageenan paw pain challenge (CAR) in male rats. (**D**) Representative traces showing action potential spiking across treatment conditions in male rats. (**E**) Depiction of the relationship between injected current and action potential firing in female rats across treatment conditions. (**F**) The cumulative number of action potentials fired across all current steps was increased by both AIE exposure and CAR in female rats. (**G**) Representative traces showing action potential spiking across treatment conditions in female rats. Data represent the mean ± SEM. *, indicates a significant difference between the related conditions; $p < 0.05$; n = 10 rats/group.

Figure 5. Optically evoked postsynaptic excitatory and inhibitory currents onto pyramidal neurons projecting from the prelimbic cortex to the ventrolateral periaqueductal gray (PrL^{PAG}). (**A**) Electrophysiological recordings were obtained from PrL^{PAG} neurons in the PrL cortex. The amplitude of optically evoked excitatory postsynaptic currents (oEPSCs) was not significantly altered by adolescent intermittent ethanol (AIE) exposure or a carrageenan paw pain challenge (CAR) in either male (**B**) or female (**F**) rats. In contrast, the amplitude of optically evoked inhibitory postsynaptic

currents (oIPSCs) was significantly reduced in both male (**C**) and female (**G**) AIE exposed rats. Carrageenan enhanced the amplitude of oIPSCs, but this increase was attenuated in AIE exposed rats. Examination of the oEPSC/oIPSC (E/I) ratios as a measure of excitatory-inhibitory balance at BLA inputs onto PrL^{PAG} neurons revealed that in AIE exposed animals, the E/I balance was significantly increase in both male (**D**) and female (**H**) rats. (**E**) Representative traces of the oEPSC and oIPSC currents recorded from male rats across all treatment groups. (**I**) Representative traces of oEPSC and oIPSC currents recorded from female rats across all treatment groups. Data represent the mean ± SEM. *, indicates a significant difference between the related conditions; $p < 0.05$; n = 8-10 rats/group.

Figure 6. Optically evoked AMPA and NMDA currents at monosynaptic inputs from the basolateral amygdala (BLA) onto pyramidal neurons projecting from the prelimbic cortex to the ventrolateral periaqueductal gray (PrL^{PAG}). (**A**) Electrophysiological recordings were obtained from PrL^{PAG} neurons in the PrL cortex. The amplitude of optically evoked AMPA currents was not altered by adolescent intermittent ethanol (AIE) exposure or a carrageenan paw pain challenge (CAR) in either male (**B**) or female (**F**) rats. Similarly, the amplitude of optically evoked NMDA currents was unchanged across all treatment conditions in both male (**C**) and female (**G**) rats. The AMPA/NMDA ratio was also not significantly altered by AIE or CAR in male (**D**) or female (**H**) rats. (**E**) Representative traces of optically evoked AMPA and NMDA currents recorded from male rats across all treatment groups. (**I**) Representative traces of optically evoked AMPA and NMDA currents recorded from female rats across all treatment groups. Data represent the mean ± SEM. n = 10 rats/group.

Figure 7. Optically evoked asynchronous excitatory postsynaptic currents (aEPSCs) at monosynaptic inputs from the basolateral amygdala (BLA) onto pyramidal neurons projecting from the prelimbic cortex to the ventrolateral periaqueductal gray (PrL^{PAG}). (**A**) Electrophysiological recordings were obtained from PrL^{PAG} neurons in the PrL cortex. When compared across treatment conditions, there were no differences in either the amplitude (**B,E**) or interevent interval (**C,F**) of aEPSCs. (**D**) Representative traces of aEPSCs recorded from male rats across all treatment groups. (**G**) Representative traces of aEPSCs recorded from female rats across all treatment groups. Data represent the mean ± SEM. On the current traces, a + indicates an asynchronous event. n = 8-10 rats/group.

Figure 8. Intrinsic excitability of prelimbic parvalbumin interneurons (PVINs). (**A**) Electrophysiological recordings were obtained from PVINs in the PrL cortex. (**B**) Depiction of the relationship between injected current and action potential firing in male rats across treatment conditions. (**C**) Adolescent intermittent ethanol (AIE) exposure reduced the cumulative number of action potentials fired across all current steps in male rats. (**D**) Representative traces showing action potential spiking across treatment conditions in male rats. (**E**) Depiction of the relationship between injected current and action potential firing in female rats across treatment conditions. (**F**) Adolescent intermittent ethanol exposure reduced the cumulative number of action potentials fired across all current steps in female rats. (**G**) Representative traces showing action potential spiking across treatment conditions in female rats. Data represent the mean ± SEM. *, indicates a significant difference between the related conditions; $p < 0.05$; n = 10 rats/group.

Figure 9. Optically evoked postsynaptic excitatory and inhibitory currents onto prelimbic parvalbumin interneurons (PVINs). (**A**) Electrophysiological recordings were obtained from PVINs in the PrL cortex. The amplitude of optically evoked excitatory postsynaptic currents (oEPSCs) onto PVINs was found to be significantly reduced by adolescent intermittent ethanol (AIE) exposure in both (**B**) male and (**F**) female rats. Quantification of the amplitude of optically evoked inhibitory postsynaptic currents (oIPSCs) revealed that oIPSCs onto PVINs were altered by AIE in a sex-

dependent manner, although post-hoc analysis did not reveal a significant difference based on any combination of sex and AIE (**C,G**). Examination of the oEPSC/oIPSC (E/I) ratios as a measure of excitatory-inhibitory balance at BLA inputs onto PVINs revealed that a carrageenan paw pain challenge (CAR) enhanced the E/I ratio at PVINs in both male (**D**) and female (**H**) rats, while AIE reduced the E/I ratio. The effect of AIE on E/I balance was greater in males (**D**) than in females (**H**). (**E**) Representative traces of the oEPSC and oIPSC currents recorded from male rats across all treatment groups. (**I**) Representative traces of oEPSC and oIPSC currents recorded from female rats across all treatment groups. Data represent the mean ± SEM. *, indicates a significant difference between the related conditions; $p < 0.05$; n = 10 rats/group.

Figure 10. Optically evoked AMPA and NMDA currents at monosynaptic inputs from the basolateral amygdala (BLA) onto prelimbic parvalbumin interneurons (PVINs). (**A**) Electrophysiological recordings were obtained from PVINs in the PrL cortex. The amplitude of optically evoked AMPA currents was increased by a carrageenan paw pain challenge (CAR) but decreased by adolescent intermittent ethanol (AIE) exposure in both male (**B**) and female (**F**) rats. Similarly, AIE reduced the amplitude of optically evoked NMDA currents in both male (**C**) and female (**G**) rats. Examination of the AMPA/NMDA ratios revealed that CAR enhanced the AMPA/NMDA ratio at BLA inputs onto prelimbic PVINs in both male (**D**) and female (**H**) rats. However, this increase was attenuated in AIE exposed rats. (**E**) Representative traces of optically evoked AMPA and NMDA currents recorded from male rats across all treatment groups. (**I**) Representative traces of optically evoked AMPA and NMDA currents recorded from female rats across all treatment groups. Data represent the mean ± SEM. *, indicates a significant difference between the related conditions; $p < 0.05$; n = 10 rats/group.

Figure 11. Optically evoked asynchronous excitatory postsynaptic currents (aEPSCs) at monosynaptic inputs from the basolateral amygdala (BLA) onto prelimbic parvalbumin interneurons (PVINs). (**A**) Electrophysiological recordings were obtained from PVINs in the PrL cortex. Adolescent intermittent ethanol (AIE) exposure was found to decrease the amplitude of aEPSCs from both male (**B**) and female (**E**) rats. The interevent interval of aEPSCs, however, was unaltered by either AIE or a carrageenan paw pain challenge (CAR) in male (**C**) and female (**F**) rats. (**D**) Representative traces of aEPSCs recorded from male rats across all treatment groups. (**G**) Representative traces of aEPSCs recorded from female rats across all treatment groups. Data represent the mean ± SEM. +, indicates an asynchronous event; *, indicates a significant difference between the related conditions; $p < 0.05$; n = 9-10 rats/group.

References

1. Riley JL, 3rd, King C. Self-report of alcohol use for pain in a multi-ethnic community sample. *J Pain*. Sep 2009;10(9):944-52. doi:10.1016/j.jpain.2009.03.005
2. Alford DP, German JS, Samet JH, Cheng DM, Lloyd-Travaglini CA, Saitz R. Primary Care Patients with Drug Use Report Chronic Pain and Self-Medicate with Alcohol and Other Drugs. *J Gen Intern Med*. May 2016;31(5):486-91. doi:10.1007/s11606-016-3586-5
3. Thompson T, Oram C, Correll CU, Tsermentseli S, Stubbs B. Analgesic Effects of Alcohol: A Systematic Review and Meta-Analysis of Controlled Experimental Studies in Healthy Participants. *J Pain*. May 2017;18(5):499-510. doi:10.1016/j.jpain.2016.11.009
4. Neddenriep B, Bagdas D, Contreras KM, et al. Pharmacological mechanisms of alcohol analgesic-like properties in mouse models of acute and chronic pain. *Neuropharmacology*. Dec 1 2019;160:107793. doi:10.1016/j.neuropharm.2019.107793
5. Jochum T, Boettger MK, Burkhardt C, Juckel G, Bar KJ. Increased pain sensitivity in alcohol withdrawal syndrome. *Eur J Pain*. Aug 2010;14(7):713-8. doi:10.1016/j.ejpain.2009.11.008
6. You DS, Hahn HA, Welsh TH, Meagher MW. Hyperalgesia after a Drinking Episode in Young Adult Binge Drinkers: A Cross-Sectional Study. *Alcohol Alcohol*. Oct 20 2020;55(6):608-615. doi:10.1093/alcalc/agaa035
7. Julian T, Glascow N, Syeed R, Zis P. Alcohol-related peripheral neuropathy: a systematic review and meta-analysis. *J Neurol*. Dec 2019;266(12):2907-2919. doi:10.1007/s00415-018-9123-1
8. Dudek I, Hajduga D, Sieńko C, et al. Alcohol-Induced Neuropathy in Chronic Alcoholism: Causes, Pathophysiology, Diagnosis, and Treatment Options. *Current Pathobiology Reports*. 2020/12/01 2020;8(4):87-97. doi:10.1007/s40139-020-00214-w
9. Dina OA, Barletta J, Chen X, et al. Key role for the epsilon isoform of protein kinase C in painful alcoholic neuropathy in the rat. *J Neurosci*. Nov 15 2000;20(22):8614-9. doi:10.1523/JNEUROSCI.20-22-08614.2000
10. Edwards S, Vendruscolo LF, Schlosburg JE, et al. Development of mechanical hypersensitivity in rats during heroin and ethanol dependence: alleviation by CRF(1) receptor antagonism. *Neuropharmacology*. Feb 2012;62(2):1142-51. doi:10.1016/j.neuropharm.2011.11.006
11. McDermott KA, Joyner KJ, Hakes JK, Okey SA, Cougle JR. Pain interference and alcohol, nicotine, and cannabis use disorder in a national sample of substance users. *Drug Alcohol Depend*. May 1 2018;186:53-59. doi:10.1016/j.drugalcdep.2018.01.011
12. Barry DT, Pilver CE, Hoff RA, Potenza MN. Pain interference and incident mood, anxiety, and substance-use disorders: findings from a representative sample of men and women in the general population. *J Psychiatr Res*. Nov 2013;47(11):1658-64. doi:10.1016/j.jpsychires.2013.08.004
13. Edlund MJ, Sullivan MD, Han X, Booth BM. Days with pain and substance use disorders: is there an association? *Clin J Pain*. Aug 2013;29(8):689-95. doi:10.1097/AJP.0b013e318270fa77
14. Chau K, Chau N. Association between untreated low back pain and injury proneness and confounding role of behavioral-health difficulties among younger adolescents: a population-based study. *Eur Spine J*. Jun 2023;32(6):2069-2077. doi:10.1007/s00586-023-07679-4
15. Hestbaek L, Leboeuf-Yde C, Kyvik KO. Are lifestyle-factors in adolescence predictors for adult low back pain? A cross-sectional and prospective study of young twins. *BMC Musculoskelet Disord*. Mar 15 2006;7(1):27. doi:10.1186/1471-2474-7-27
16. Horn-Hofmann C, Trost Z, Hublet A, Mrug S, Van Damme J, Vervoort T. The Relationship Between Pain Severity and Alcohol Use Among School-Aged Children and Adolescents: The Moderating Role of Drinking Motives. *Pain Med*. Feb 1 2018;19(2):284-296. doi:10.1093/pm/pnx016

17. Pascale A, Stephenson M, Barr P, et al. Exploring the relationships between adolescent alcohol misuse and later life health outcomes. *Alcohol Clin Exp Res*. Sep 2022;46(9):1753-1765. doi:10.1111/acer.14917
18. Khan KM, Bierlein-De La Rosa G, Biggerstaff N, et al. Adolescent ethanol drinking promotes hyperalgesia, neuroinflammation and serotonergic deficits in mice that persist into adulthood. *Brain Behav Immun*. Jan 2023;107:419-431. doi:10.1016/j.bbi.2022.07.160
19. Kelley AM, Del Valle EJ, Zaman S, Karkhanis AN. Adolescent ethanol exposure promotes mechanical allodynia and alters dopamine transmission in the nucleus accumbens shell. *Pain*. Nov 14 2023:10.1097/j.pain.0000000000003097. doi:10.1097/j.pain.0000000000003097
20. Secci ME, Kelley LK, Avegno EM, et al. Adolescent Alcohol Exposure Produces Sex-Specific Long-term Hyperalgesia via Changes in Central Amygdala Circuit Function. *Biol Psychiatry*. Feb 1 2024;95(3):207-219. doi:10.1016/j.biopsych.2023.09.006
21. Bertagna NB, Wilson L, Bailey CK, Cruz FC, Albrechet-Souza L, Wills TA. Long-lasting mechanical hypersensitivity and CRF receptor type-1 neuron activation in the BNST following adolescent ethanol exposure. *Alcohol Clin Exp Res (Hoboken)*. Jan 2024;48(1):48-57. doi:10.1111/acer.15228
22. Ong WY, Stohler CS, Herr DR. Role of the Prefrontal Cortex in Pain Processing. *Mol Neurobiol*. Feb 2019;56(2):1137-1166. doi:10.1007/s12035-018-1130-9
23. Bastuji H, Frot M, Perchet C, Magnin M, Garcia-Larrea L. Pain networks from the inside: Spatiotemporal analysis of brain responses leading from nociception to conscious perception. *Hum Brain Mapp*. Dec 2016;37(12):4301-4315. doi:10.1002/hbm.23310
24. Garcia-Larrea L, Peyron R. Pain matrices and neuropathic pain matrices: a review. *Pain*. Dec 2013;154 Suppl 1:S29-S43. doi:10.1016/j.pain.2013.09.001
25. Cunningham MG, Bhattacharyya S, Benes FM. Amygdalo-cortical sprouting continues into early adulthood: implications for the development of normal and abnormal function during adolescence. *J Comp Neurol*. Nov 11 2002;453(2):116-30. doi:10.1002/cne.10376
26. Gabbott PL, Warner TA, Busby SJ. Amygdala input monosynaptically innervates parvalbumin immunoreactive local circuit neurons in rat medial prefrontal cortex. *Neuroscience*. 2006/01/01/ 2006;139(3):1039-48. doi:10.1016/j.neuroscience.2006.01.026
27. Krettek JE, Price JL. Projections from the amygdaloid complex to the cerebral cortex and thalamus in the rat and cat. *J Comp Neurol*. Apr 15 1977;172(4):687-722. doi:10.1002/cne.901720408
28. An X, Bandler R, Ongur D, Price JL. Prefrontal cortical projections to longitudinal columns in the midbrain periaqueductal gray in macaque monkeys. *J Comp Neurol*. Nov 30 1998;401(4):455-79.
29. Floyd NS, Price JL, Ferry AT, Keay KA, Bandler R. Orbitomedial prefrontal cortical projections to distinct longitudinal columns of the periaqueductal gray in the rat. *J Comp Neurol*. Jul 10 2000;422(4):556-78. doi:10.1002/1096-9861(20000710)422:4<556::aid-cne6>3.0.co;2-u
30. McGarry LM, Carter AG. Inhibitory Gating of Basolateral Amygdala Inputs to the Prefrontal Cortex. *J Neurosci*. Sep 7 2016;36(36):9391-406. doi:10.1523/JNEUROSCI.0874-16.2016
31. Cheriyan J, Kaushik MK, Ferreira AN, Sheets PL. Specific Targeting of the Basolateral Amygdala to Projectionally Defined Pyramidal Neurons in Prelimbic and Infralimbic Cortex. *eNeuro*. Mar-Apr 2016;3(2)doi:10.1523/ENEURO.0002-16.2016
32. Huang J, Gadotti VM, Chen L, et al. A neuronal circuit for activating descending modulation of neuropathic pain. *Nat Neurosci*. Oct 2019;22(10):1659-1668. doi:10.1038/s41593-019-0481-5
33. Gadotti VM, Zhang Z, Huang J, Zamponi GW. Analgesic effects of optogenetic inhibition of basolateral amygdala inputs into the prefrontal cortex in nerve injured female mice. *Mol Brain*. Dec 4 2019;12(1):105. doi:10.1186/s13041-019-0529-1

34. Dilgen J, Tejeda HA, O'Donnell P. Amygdala inputs drive feedforward inhibition in the medial prefrontal cortex. *J Neurophysiol*. Jul 2013;110(1):221-9. doi:10.1152/jn.00531.2012
35. Zhang Z, Gadotti VM, Chen L, Souza IA, Stemkowski PL, Zamponi GW. Role of Prelimbic GABAergic Circuits in Sensory and Emotional Aspects of Neuropathic Pain. *Cell Rep*. Aug 4 2015;12(5):752-9. doi:10.1016/j.celrep.2015.07.001
36. Yin JB, Liang SH, Li F, et al. dmPFC-vlPAG projection neurons contribute to pain threshold maintenance and antianxiety behaviors. *J Clin Invest*. Dec 1 2020;130(12):6555-6570. doi:10.1172/JCI127607
37. Drake RA, Steel KA, Apps R, Lumb BM, Pickering AE. Loss of cortical control over the descending pain modulatory system determines the development of the neuropathic pain state in rats. *Elife*. Feb 8 2021;10:e65156. doi:10.7554/eLife.65156
38. Gao F, Huang J, Huang GB, et al. Elevated prelimbic cortex-to-basolateral amygdala circuit activity mediates comorbid anxiety-like behaviors associated with chronic pain. *J Clin Invest*. May 1 2023;133(9)doi:10.1172/JCI166356
39. Fan XC, Fu S, Liu FY, Cui S, Yi M, Wan Y. Hypersensitivity of Prelimbic Cortex Neurons Contributes to Aggravated Nociceptive Responses in Rats With Experience of Chronic Inflammatory Pain. Original Research. *Front Mol Neurosci*. 2018-March-22 2018;11:85. doi:10.3389/fnmol.2018.00085
40. Crews FT, Robinson DL, Chandler LJ, et al. Mechanisms of Persistent Neurobiological Changes Following Adolescent Alcohol Exposure: NADIA Consortium Findings. *Alcohol Clin Exp Res*. Sep 2019;43(9):1806-1822. doi:10.1111/acer.14154
41. Spear LP. Effects of adolescent alcohol consumption on the brain and behaviour. *Nat Rev Neurosci*. Apr 2018;19(4):197-214. doi:10.1038/nrn.2018.10
42. Spear LP. The adolescent brain and age-related behavioral manifestations. *Neurosci Biobehav Rev*. Jun 2000;24(4):417-63. doi:10.1016/s0149-7634(00)00014-2
43. Petanjek Z, Judas M, Simic G, et al. Extraordinary neoteny of synaptic spines in the human prefrontal cortex. *Proc Natl Acad Sci U S A*. Aug 9 2011;108(32):13281-6. doi:10.1073/pnas.1105108108
44. Rakic P, Bourgeois J-P, Goldman-Rakic PS. Synaptic development of the cerebral cortex: implications for learning, memory, and mental illness. In: Van Pelt J, Corner MA, Uylings HBM, Lopes Da Silva FH, eds. *Progress in Brain Research*. Elsevier; 1994:227-243.
45. Koss WA, Belden CE, Hristov AD, Juraska JM. Dendritic remodeling in the adolescent medial prefrontal cortex and the basolateral amygdala of male and female rats. *Synapse*. Feb 2014;68(2):61-72. doi:10.1002/syn.21716
46. Mallya AP, Wang HD, Lee HNR, Deutch AY. Microglial Pruning of Synapses in the Prefrontal Cortex During Adolescence. *Cereb Cortex*. Apr 1 2019;29(4):1634-1643. doi:10.1093/cercor/bhy061
47. Drzewiecki CM, Willing J, Juraska JM. Synaptic number changes in the medial prefrontal cortex across adolescence in male and female rats: A role for pubertal onset. *Synapse*. Sep 2016;70(9):361-8. doi:10.1002/syn.21909
48. Insel TR, Miller LP, Gelhard RE. The ontogeny of excitatory amino acid receptors in rat forebrain--I. N-methyl-D-aspartate and quisqualate receptors. *Neuroscience*. 1990/01/01/ 1990;35(1):31-43. doi:10.1016/0306-4522(90)90117-m
49. Murphy KM, Tcharnaia L, Beshara SP, Jones DG. Cortical development of AMPA receptor trafficking proteins. *Front Mol Neurosci*. 2012;5:65. doi:10.3389/fnmol.2012.00065
50. Flores-Barrera E, Thomases DR, Heng LJ, Cass DK, Caballero A, Tseng KY. Late adolescent expression of GluN2B transmission in the prefrontal cortex is input-specific and requires postsynaptic protein kinase A and D1 dopamine receptor signaling. *Biol Psychiatry*. Mar 15 2014;75(6):508-16. doi:10.1016/j.biopsych.2013.07.033

51. Cunningham MG, Bhattacharyya S, Benes FM. Increasing Interaction of amygdalar afferents with GABAergic interneurons between birth and adulthood. *Cereb Cortex*. Jul 2008;18(7):1529-35. doi:10.1093/cercor/bhm183
52. Caballero A, Flores-Barrera E, Cass DK, Tseng KY. Differential regulation of parvalbumin and calretinin interneurons in the prefrontal cortex during adolescence. *Brain Struct Funct*. Jan 2014;219(1):395-406. doi:10.1007/s00429-013-0508-8
53. Caballero A, Orozco A, Tseng KY. Developmental regulation of excitatory-inhibitory synaptic balance in the prefrontal cortex during adolescence. *Semin Cell Dev Biol*. Oct 2021;118:60-63. doi:10.1016/j.semcdb.2021.02.008
54. Klune CB, Jin B, DeNardo LA. Linking mPFC circuit maturation to the developmental regulation of emotional memory and cognitive flexibility. *Elife*. May 5 2021;10:e64567. doi:10.7554/eLife.64567
55. Cass DK, Flores-Barrera E, Thomases DR, Vital WF, Caballero A, Tseng KY. CB1 cannabinoid receptor stimulation during adolescence impairs the maturation of GABA function in the adult rat prefrontal cortex. Article. *Mol Psychiatry*. May 2014;19(5):536-43. doi:10.1038/mp.2014.14
56. Trantham-Davidson H, Centanni SW, Garr SC, et al. Binge-Like Alcohol Exposure During Adolescence Disrupts Dopaminergic Neurotransmission in the Adult Prelimbic Cortex. *Neuropsychopharmacology*. Apr 2017;42(5):1024-1036. doi:10.1038/npp.2016.190
57. Centanni SW, Burnett EJ, Trantham-Davidson H, Chandler LJ. Loss of delta-GABAA receptor-mediated tonic currents in the adult prelimbic cortex following adolescent alcohol exposure. *Addict Biol*. May 2017;22(3):616-628. doi:10.1111/adb.12353
58. Salling MC, Skelly MJ, Avegno E, et al. Alcohol Consumption during Adolescence in a Mouse Model of Binge Drinking Alters the Intrinsic Excitability and Function of the Prefrontal Cortex through a Reduction in the Hyperpolarization-Activated Cation Current. *J Neurosci*. Jul 4 2018;38(27):6207-6222. doi:10.1523/JNEUROSCI.0550-18.2018
59. Galaj E, Guo C, Huang D, Ranaldi R, Ma YY. Contrasting effects of adolescent and early-adult ethanol exposure on prelimbic cortical pyramidal neurons. *Drug Alcohol Depend*. Nov 1 2020;216:108309. doi:10.1016/j.drugalcdep.2020.108309
60. Gass JT, Glen WB, Jr., McGonigal JT, et al. Adolescent alcohol exposure reduces behavioral flexibility, promotes disinhibition, and increases resistance to extinction of ethanol self-administration in adulthood. *Neuropsychopharmacology*. Oct 2014;39(11):2570-83. doi:10.1038/npp.2014.109
61. Chandler LJ, Vaughan DT, Gass JT. Adolescent Alcohol Exposure Results in Sex-specific Alterations in Conditioned Fear Learning and Memory in Adulthood. *Front Pharmacol*. 2022;13:837657. doi:10.3389/fphar.2022.837657
62. Barker JM, Bryant KG, Osborne JI, Chandler LJ. Age and Sex Interact to Mediate the Effects of Intermittent, High-Dose Ethanol Exposure on Behavioral Flexibility. *Front Pharmacol*. 2017;8:450. doi:10.3389/fphar.2017.00450
63. Glover EJ, Khan F, Clayton-Stiglbauer K, Chandler LJ. Impact of sex, strain, and age on blood ethanol concentration and behavioral signs of intoxication during ethanol vapor exposure. *Neuropharmacology*. Feb 15 2021;184:108393. doi:10.1016/j.neuropharm.2020.108393
64. Trantham-Davidson H, Burnett EJ, Gass JT, et al. Chronic alcohol disrupts dopamine receptor activity and the cognitive function of the medial prefrontal cortex. *J Neurosci*. Mar 5 2014;34(10):3706-18. doi:10.1523/JNEUROSCI.0623-13.2014
65. Petreanu L, Mao T, Sternson SM, Svoboda K. The subcellular organization of neocortical excitatory connections. *Nature*. Feb 26 2009;457(7233):1142-5. doi:10.1038/nature07709
66. Cho JH, Deisseroth K, Bolshakov VY. Synaptic encoding of fear extinction in mPFC-amygdala circuits. *Neuron*. Dec 18 2013;80(6):1491-507. doi:10.1016/j.neuron.2013.09.025

67. Dodge FA, Jr., Miledi R, Rahamimoff R. Strontium and quantal release of transmitter at the neuromuscular junction. *J Physiol*. Jan 1969;200(1):267-83. doi:10.1113/jphysiol.1969.sp008692
68. Choi S, Lovinger DM. Decreased frequency but not amplitude of quantal synaptic responses associated with expression of corticostriatal long-term depression. *J Neurosci*. Nov 1 1997;17(21):8613-20. doi:10.1523/JNEUROSCI.17-21-08613.1997
69. Xu-Friedman MA, Regehr WG. Probing fundamental aspects of synaptic transmission with strontium. *J Neurosci*. Jun 15 2000;20(12):4414-22. doi:10.1523/JNEUROSCI.20-12-04414.2000
70. Benitz KF, Hall LM. Local morphological response following a single subcutaneous injection of carrageenin in the rat. *Proc Soc Exp Biol Med*. Nov 1959;102:442-5. doi:10.3181/00379727-102-25278
71. Winter CA, Risley EA, Nuss GW. Carrageenin-induced edema in hind paw of the rat as an assay for antiiflammatory drugs. *Proc Soc Exp Biol Med*. Dec 1962;111(3):544-7. doi:10.3181/00379727-111-27849
72. Vazquez E, Navarro M, Salazar Y, et al. Systemic changes following carrageenan-induced paw inflammation in rats. *Inflamm Res*. May 2015;64(5):333-42. doi:10.1007/s00011-015-0814-0
73. Neves AF, Farias FH, de Magalhães SF, et al. Peripheral Inflammatory Hyperalgesia Depends on P2X7 Receptors in Satellite Glial Cells. *Frontiers in Physiology*. 2020;11:473. doi:10.3389/fphys.2020.00473
74. Yang PY, Tsaur ML. NS5806 reduces carrageenan-evoked inflammation by suppressing extracellular signal-regulated kinase activation in primary sensory neurons and immune cells. *Eur J Pain*. Sep 2023;27(8):927-939. doi:10.1002/ejp.2123
75. de Oliveira BMT, Telles T, Lomba LA, Correia D, Zampronio AR. Effects of binge-like ethanol exposure during adolescence on the hyperalgesia observed during sickness syndrome in rats. *Pharmacol Biochem Behav*. Sep 2017;160:63-69. doi:10.1016/j.pbb.2017.08.004
76. Obray JD, Landin JD, Vaughan DT, Scofield MD, Chandler LJ. Adolescent alcohol exposure reduces dopamine 1 receptor modulation of prelimbic neurons projecting to the nucleus accumbens and basolateral amygdala. *Addict Neurosci*. Dec 2022;4doi:10.1016/j.addicn.2022.100044
77. Du X, Serena K, Hwang WJ, et al. Prefrontal cortical parvalbumin and somatostatin expression and cell density increase during adolescence and are modified by BDNF and sex. *Mol Cell Neurosci*. Apr 2018;88:177-188. doi:10.1016/j.mcn.2018.02.001
78. Koppensteiner P, Von Itter R, Melani R, Galvin C, Lee FS, Ninan I. Diminished Fear Extinction in Adolescents Is Associated With an Altered Somatostatin Interneuron-Mediated Inhibition in the Infralimbic Cortex. *Biol Psychiatry*. Nov 1 2019;86(9):682-692. doi:10.1016/j.biopsych.2019.04.035
79. Sicher AR, Starnes WD, Griffith KR, et al. Adolescent binge drinking leads to long-lasting changes in cortical microcircuits in mice. *Neuropharmacology*. Aug 15 2023;234:109561. doi:10.1016/j.neuropharm.2023.109561
80. Cummings KA, Clem RL. Prefrontal somatostatin interneurons encode fear memory. *Nat Neurosci*. Jan 2020;23(1):61-74. doi:10.1038/s41593-019-0552-7
81. Qi X, Cui K, Zhang Y, et al. A nociceptive neuronal ensemble in the dorsomedial prefrontal cortex underlies pain chronicity. *Cell Rep*. Dec 13 2022;41(11):111833. doi:10.1016/j.celrep.2022.111833
82. Guo Y, Song Y, Cao F, et al. Ventrolateral periaqueductal gray GABAergic neurons promote arousal of sevoflurane anesthesia through cortico-midbrain circuit. *iScience*. 2023/08/14/ 2023:107486. doi:10.1016/j.isci.2023.107486
83. Samineni VK, Grajales-Reyes JG, Copits BA, et al. Divergent Modulation of Nociception by Glutamatergic and GABAergic Neuronal Subpopulations in the Periaqueductal Gray. *eNeuro*. Mar-Apr 2017;4(2)doi:10.1523/ENEURO.0129-16.2017

84. Wu XB, Liang B, Gao YJ. The increase of intrinsic excitability of layer V pyramidal cells in the prelimbic medial prefrontal cortex of adult mice after peripheral inflammation. *Neurosci Lett*. Jan 12 2016;611:40-5. doi:10.1016/j.neulet.2015.11.030
85. Cheriyan J, Sheets PL. Altered Excitability and Local Connectivity of mPFC-PAG Neurons in a Mouse Model of Neuropathic Pain. *J Neurosci*. May 16 2018;38(20):4829-4839. doi:10.1523/JNEUROSCI.2731-17.2018
86. Ji G, Sun H, Fu Y, et al. Cognitive impairment in pain through amygdala-driven prefrontal cortical deactivation. *J Neurosci*. Apr 14 2010;30(15):5451-64. doi:10.1523/JNEUROSCI.0225-10.2010
87. Dannenhoffer CA, Gomez AA, Macht VA, et al. Impact of adolescent intermittent ethanol exposure on interneurons and their surrounding perineuronal nets in adulthood. *Alcohol Clin Exp Res*. May 2022;46(5):759-769. doi:10.1111/acer.14810
88. Pizzorusso T, Medini P, Berardi N, Chierzi S, Fawcett JW, Maffei L. Reactivation of ocular dominance plasticity in the adult visual cortex. *Science*. Nov 8 2002;298(5596):1248-51. doi:10.1126/science.1072699
89. Balmer TS, Carels VM, Frisch JL, Nick TA. Modulation of perineuronal nets and parvalbumin with developmental song learning. *J Neurosci*. Oct 14 2009;29(41):12878-85. doi:10.1523/JNEUROSCI.2974-09.2009
90. Cornez G, Collignon C, Muller W, Cornil CA, Ball GF, Balthazart J. Development of Perineuronal Nets during Ontogeny Correlates with Sensorimotor Vocal Learning in Canaries. *eNeuro*. Mar/Apr 2020;7(2)doi:10.1523/ENEURO.0361-19.2020
91. Rozeske RR, Jercog D, Karalis N, et al. Prefrontal-Periaqueductal Gray-Projecting Neurons Mediate Context Fear Discrimination. *Neuron*. Feb 21 2018;97(4):898-910 e6. doi:10.1016/j.neuron.2017.12.044
92. Johnson SB, Lingg RT, Skog TD, et al. Activity in a prefrontal-periaqueductal gray circuit overcomes behavioral and endocrine features of the passive coping stress response. *Proc Natl Acad Sci U S A*. Nov 2022;119(44):e2210783119. doi:10.1073/pnas.2210783119

Figure 1

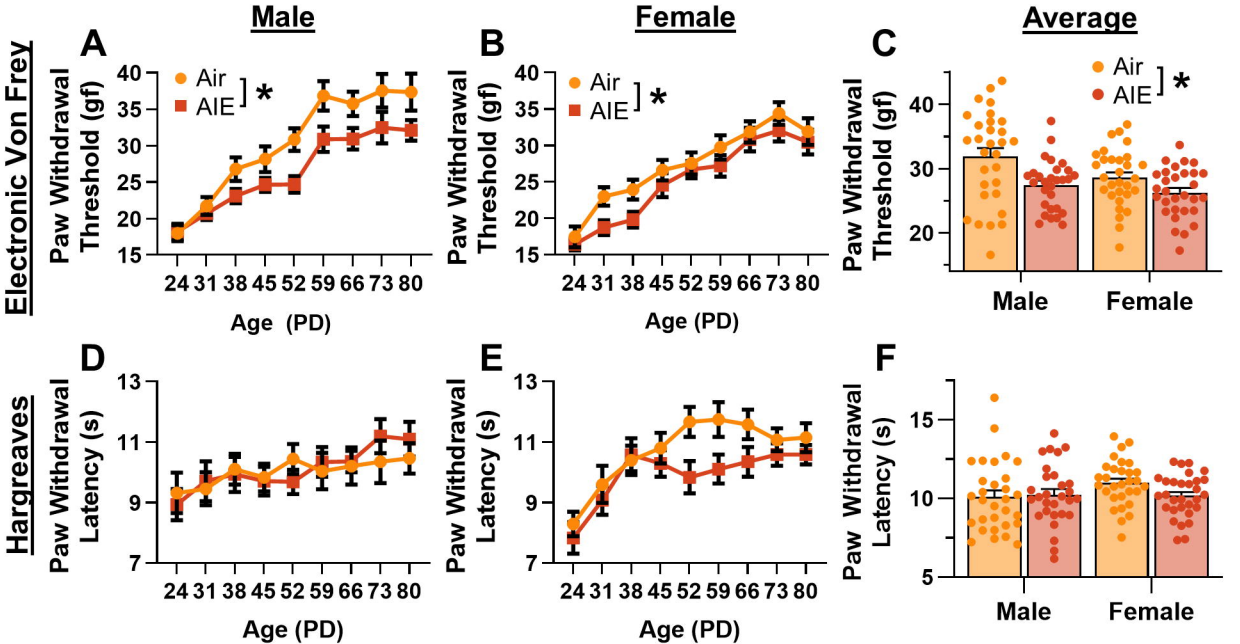
Male
Female
Average
Electronic Von Frey
Hargreaves
A
B
C
D
E
F
Air
AIE
*
Paw Withdrawal Threshold (gf)
Paw Withdrawal Latency (s)
Age (PD)
24 31 38 45 52 59 66 73 80
Male
Female

Figure 2

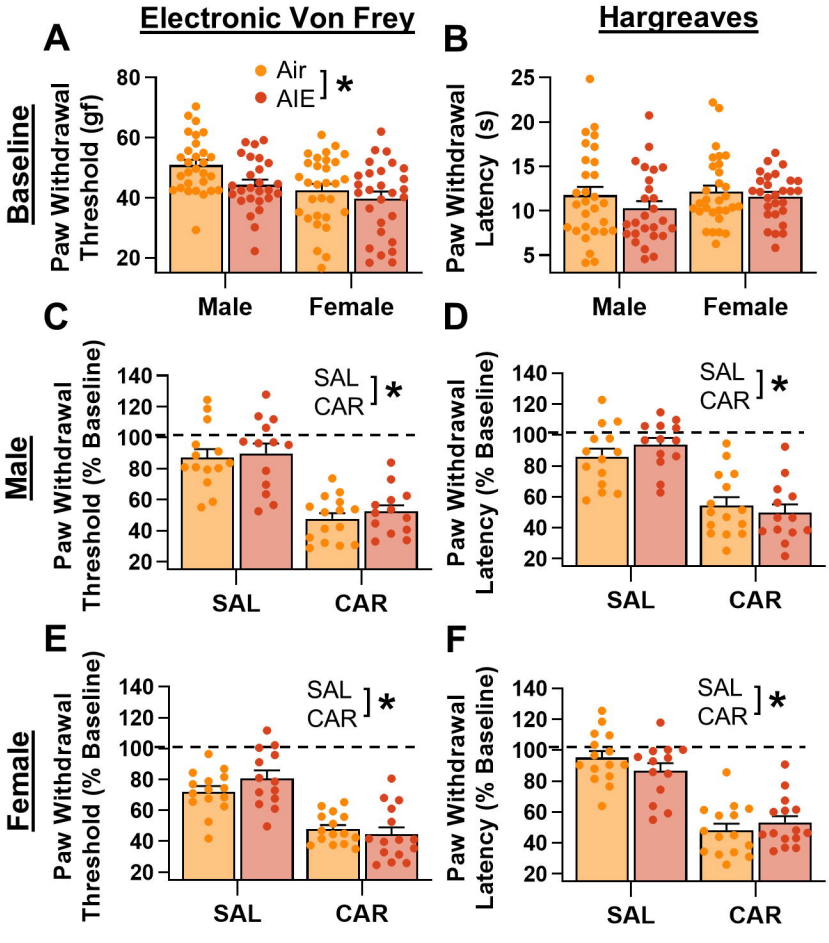
Electronic Von Frey
Hargreaves
A
B
C
D
E
F
Baseline
Male
Female
Air
AIE
*
Paw Withdrawal Threshold (gf)
Paw Withdrawal Latency (s)
Paw Withdrawal Threshold (% Baseline)
Paw Withdrawal Latency (% Baseline)
SAL
CAR
Male
Female

Figure 3

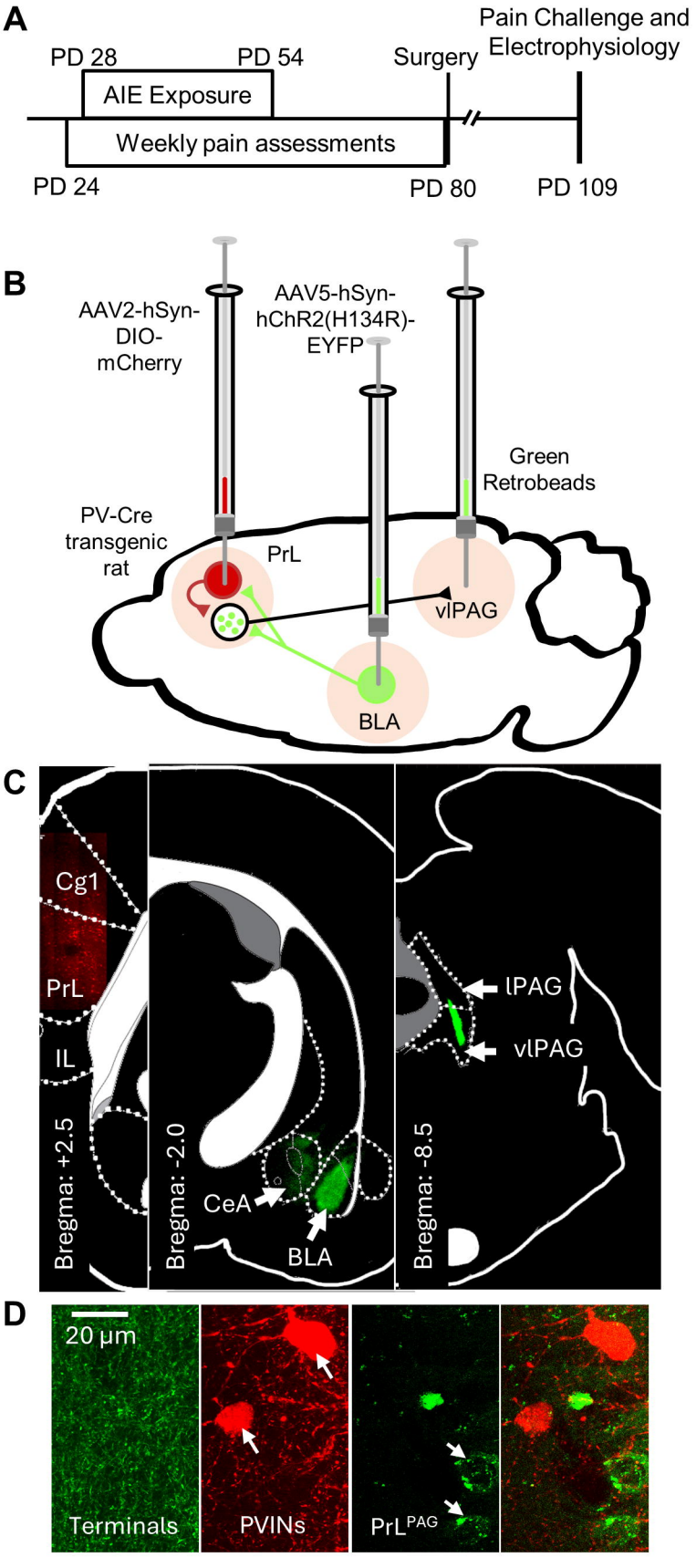
A
PD 28
PD 54
Surgery
Pain Challenge and Electrophysiology
AIE Exposure
Weekly pain assessments
PD 24
PD 80
PD 109
B
AAV2-hSyn-DIO-mCherry
AAV5-hSyn-hChR2(H134R)-EYFP
Green Retrobeads
PV-Cre transgenic rat
PrL
vlPAG
BLA
C
Cg1
PrL
IL
Bregma: +2.5
Bregma: -2.0
CeA
BLA
lPAG
vlPAG
Bregma: -8.5
D
20 µm
Terminals
PVINs
PrL^PAG

Figure 4

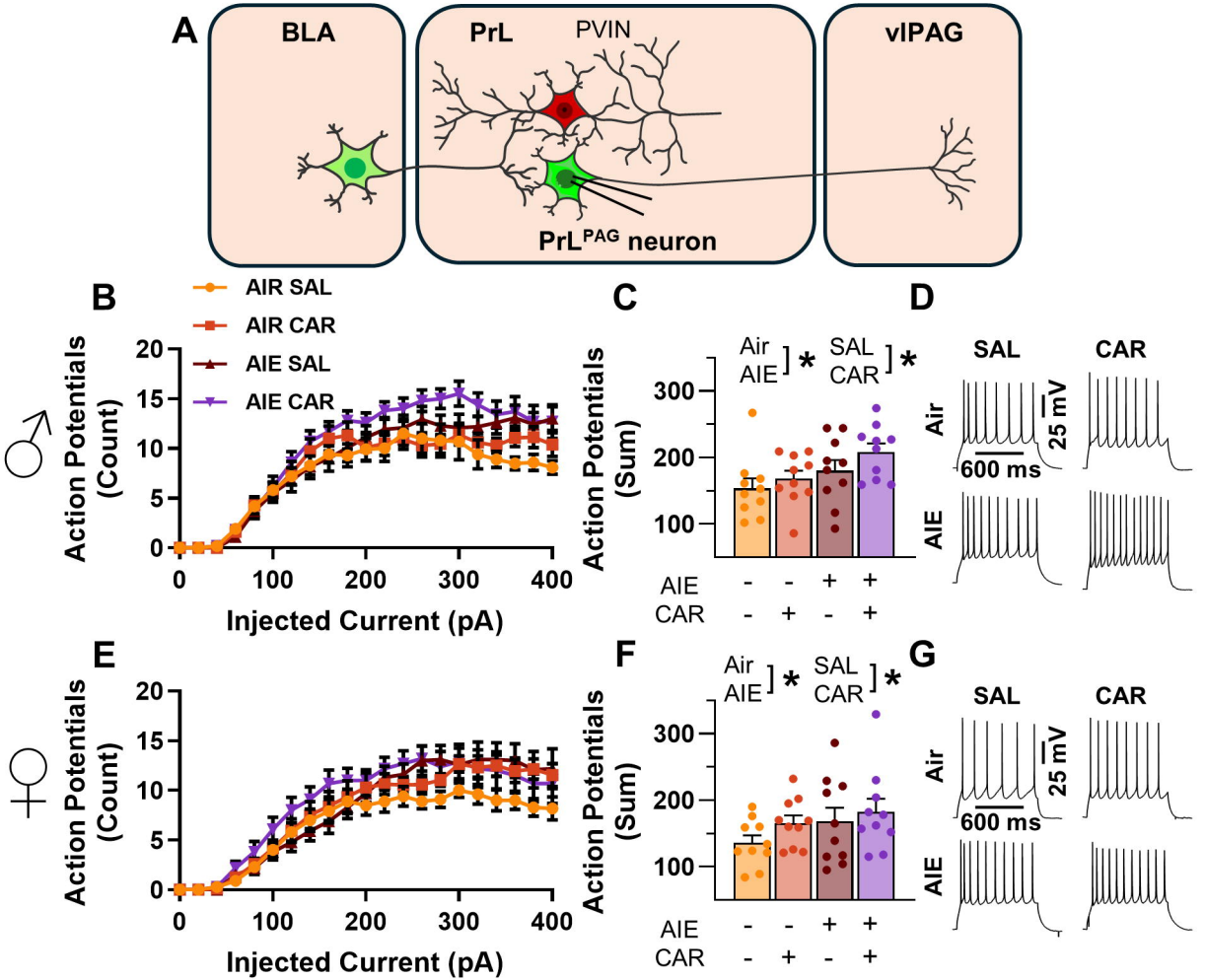
A
BLA
PrL
PVIN
vlPAG
PrL^PAG neuron
B
AIR SAL
AIR CAR
AIE SAL
AIE CAR
Action Potentials (Count)
Injected Current (pA)
C
Action Potentials (Sum)
Air
AIE
SAL
CAR
AIE
CAR
D
SAL
CAR
Air
AIE
25 mV
600 ms
E
F
G

Figure 5

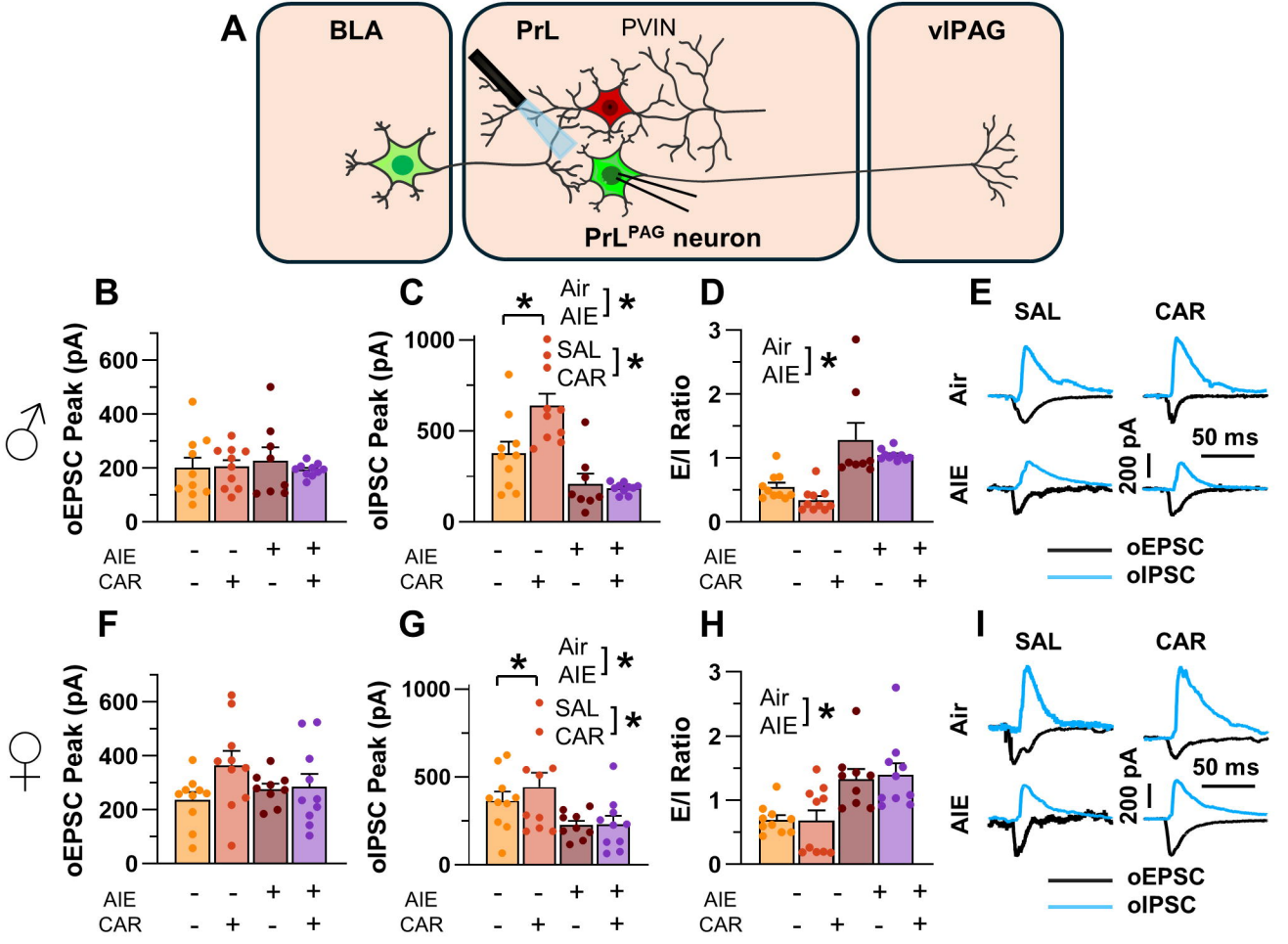
A
BLA
PrL
PVIN
vlPAG
PrL^PAG neuron
B
C
D
E
F
G
H
I
♂
♀
oEPSC Peak (pA)
oIPSC Peak (pA)
E/I Ratio
AIE
CAR
Air
SAL
oEPSC
oIPSC
50 ms
200 pA

Figure 6

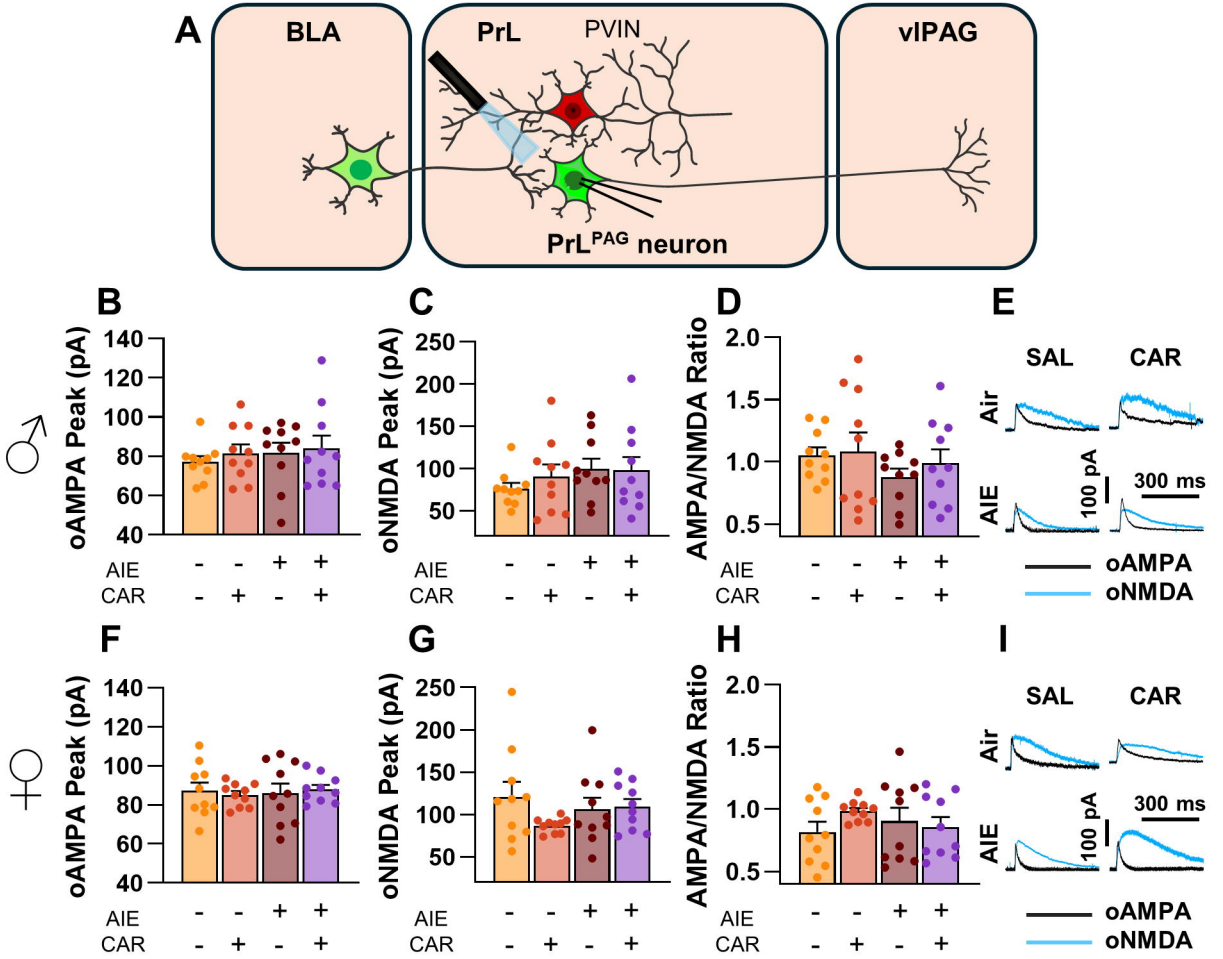
A
BLA
PrL
PVIN
vlPAG
PrL^PAG neuron
B
C
D
E
♂
oAMPA Peak (pA)
oNMDA Peak (pA)
AMPA/NMDA Ratio
AIE
CAR
SAL
CAR
Air
AIE
100 pA
300 ms
oAMPA
oNMDA
F
G
H
I
♀

Figure 7

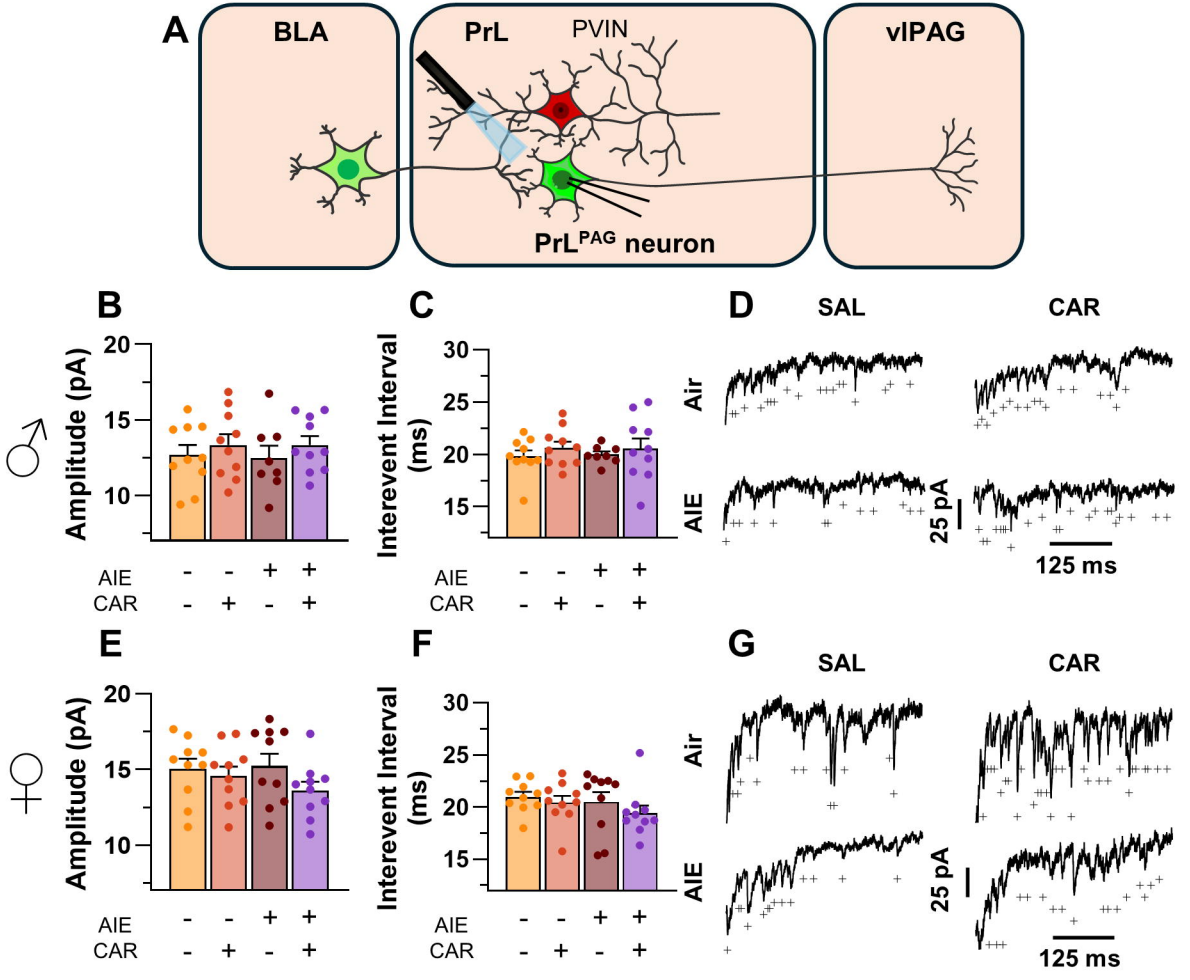
A
BLA
PrL
PVIN
vlPAG
PrL^PAG neuron
B
Amplitude (pA)
20
15
10
AIE - - + +
CAR - + - +
C
Interevent Interval (ms)
30
25
20
15
AIE - - + +
CAR - + - +
D
SAL
CAR
Air
AIE
25 pA
125 ms
E
Amplitude (pA)
20
15
10
AIE - - + +
CAR - + - +
F
Interevent Interval (ms)
30
25
20
15
AIE - - + +
CAR - + - +
G
SAL
CAR
Air
AIE
25 pA
125 ms

Figure 8

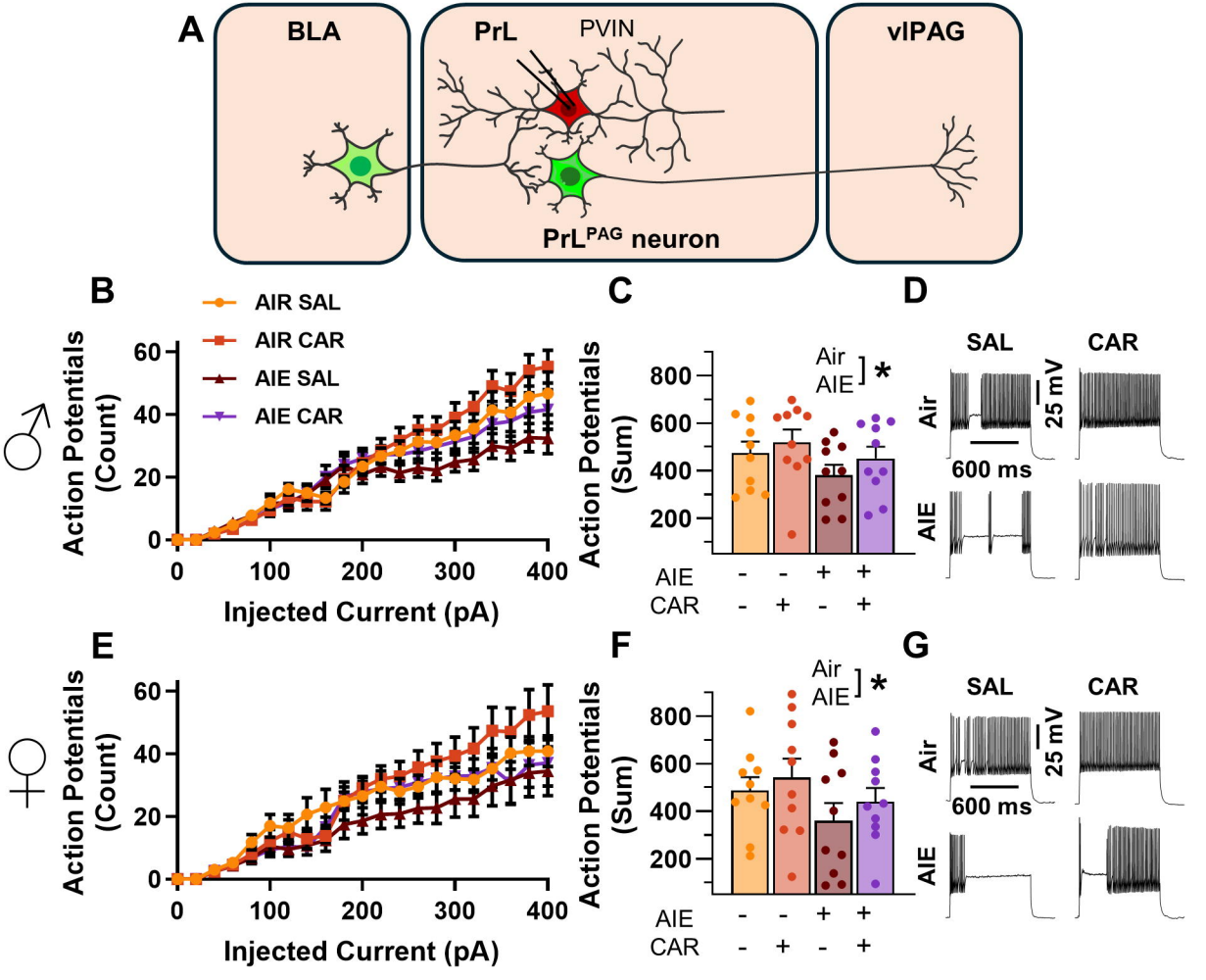
A
BLA
PrL
PVIN
vlPAG
PrL^PAG neuron
B
AIR SAL
AIR CAR
AIE SAL
AIE CAR
Action Potentials (Count)
Injected Current (pA)
C
Action Potentials (Sum)
Air
AIE
*
AIE
CAR
D
SAL
CAR
Air
AIE
25 mV
600 ms
E
F
G

Figure 9

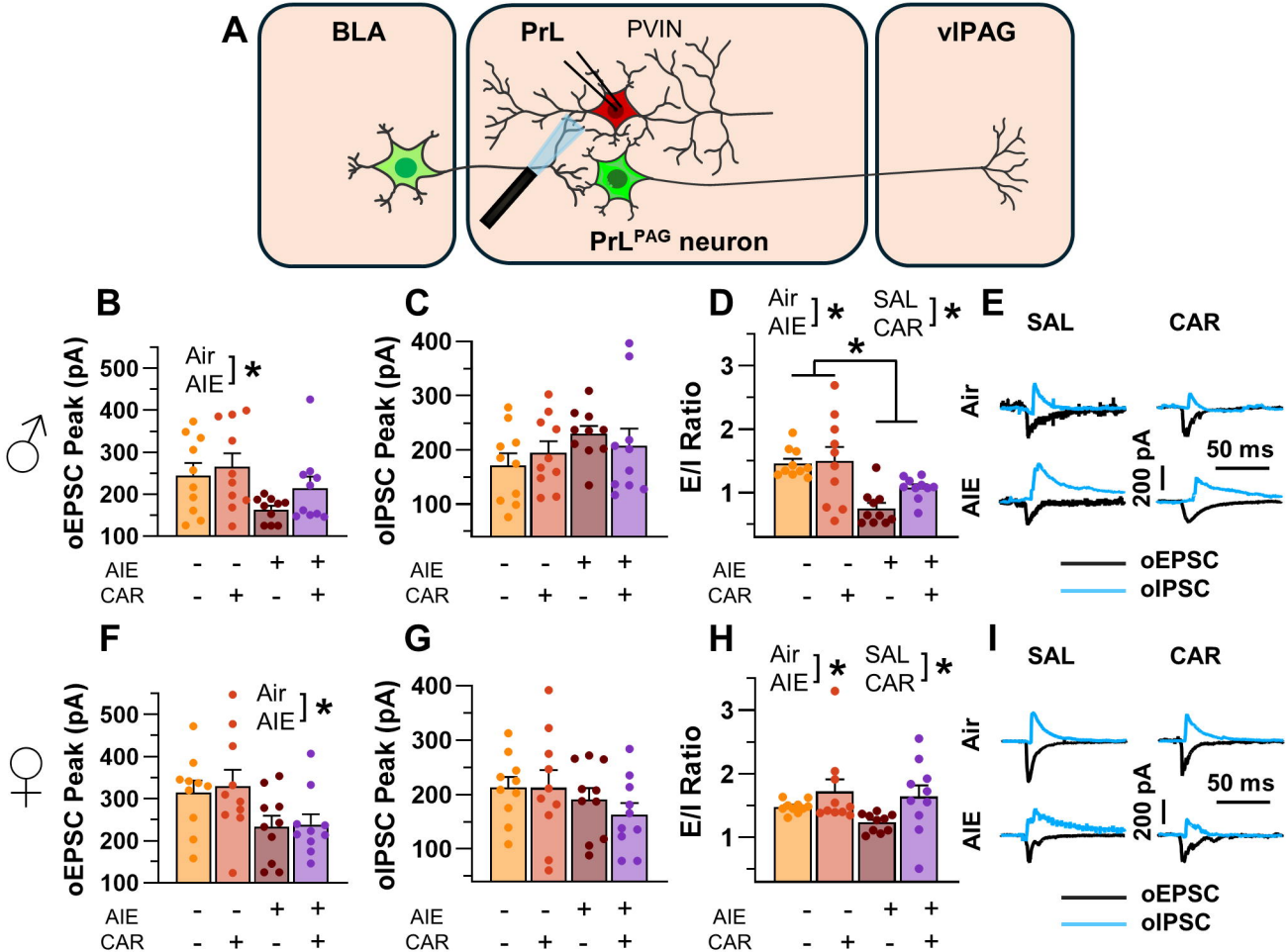
A
BLA
PrL
PVIN
vlPAG
PrL^PAG neuron
B
C
D
E
F
G
H
I
♂
♀
oEPSC Peak (pA)
oIPSC Peak (pA)
E/I Ratio
Air
AIE
SAL
CAR
AIE
CAR
50 ms
200 pA
oEPSC
oIPSC

Figure 10

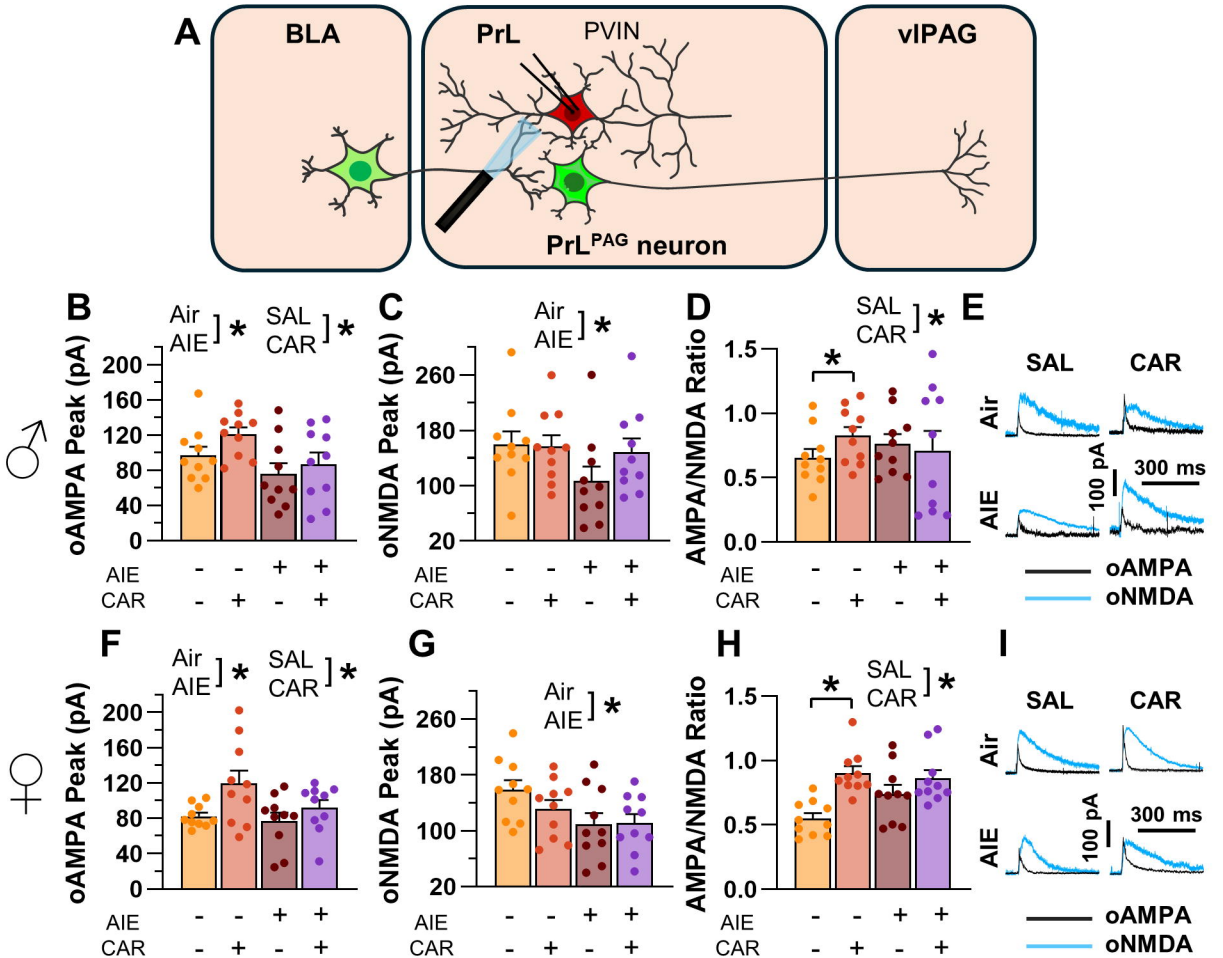
A
BLA
PrL
PVIN
vlPAG
PrL^PAG neuron
B
C
D
E
F
G
H
I
♂
♀
oAMPA Peak (pA)
oNMDA Peak (pA)
AMPA/NMDA Ratio
Air
AIE
SAL
CAR
AIE
CAR
SAL
CAR
Air
AIE
100 pA
300 ms
oAMPA
oNMDA

Figure 11

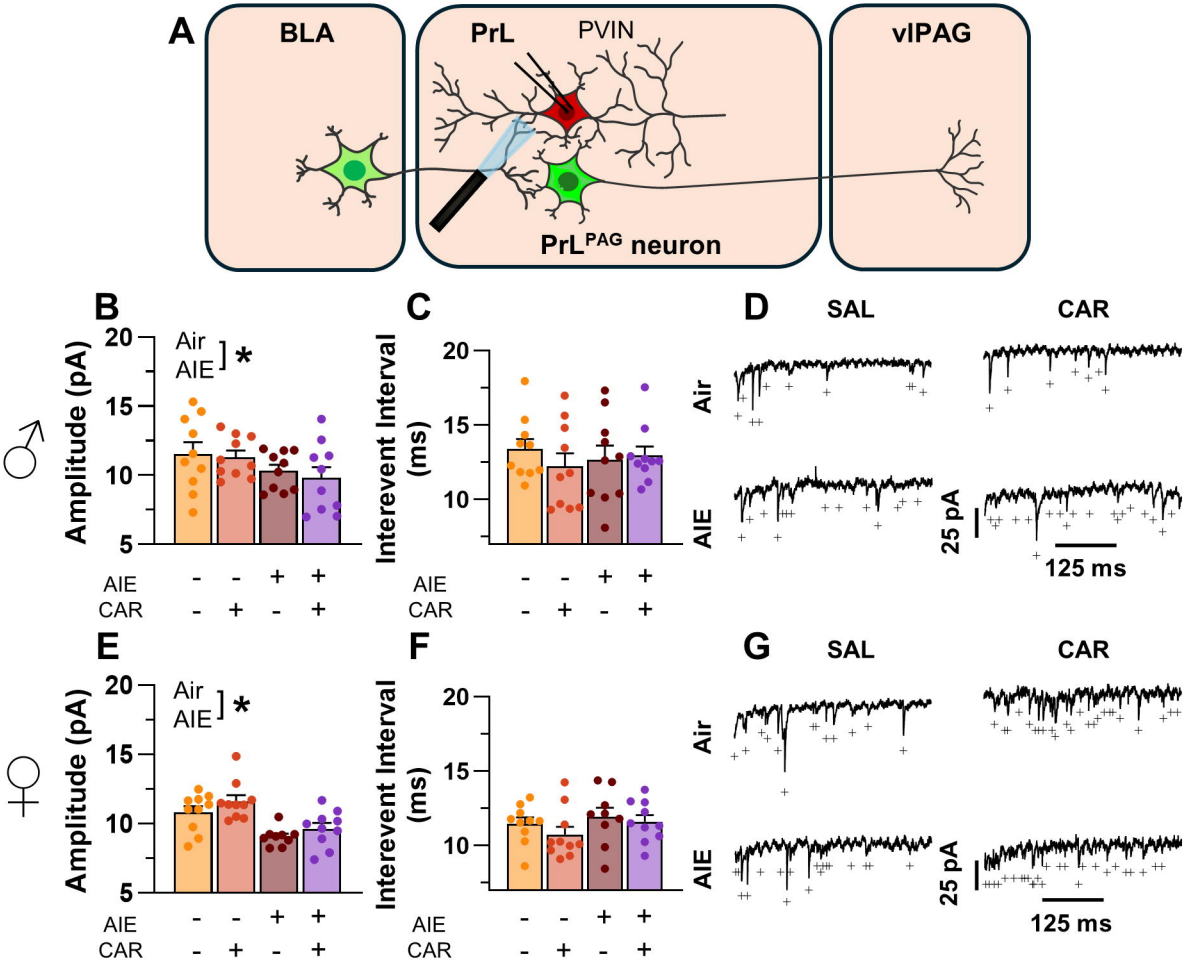
A
BLA
PrL
PVIN
vlPAG
PrL^PAG neuron
B
C
D
SAL
CAR
Air
AIE
Amplitude (pA)
Interevent Interval (ms)
AIE
CAR
25 pA
125 ms
E
F
G
♂
♀